



HAL
open science

The four cysteine residues in the second extracellular loop of the human adenosine A receptor: role in ligand binding and receptor function

Anke C. Schiedel, Sonja Hinz, Dominik Thimm, Farag Sherbiny, Thomas Borrmann, Astrid Maass, Christa E. Müller

► To cite this version:

Anke C. Schiedel, Sonja Hinz, Dominik Thimm, Farag Sherbiny, Thomas Borrmann, et al.. The four cysteine residues in the second extracellular loop of the human adenosine A receptor: role in ligand binding and receptor function. *Biochemical Pharmacology*, 2011, 82 (4), pp.389. 10.1016/j.bcp.2011.05.008 . hal-00718035

HAL Id: hal-00718035

<https://hal.science/hal-00718035>

Submitted on 16 Jul 2012

HAL is a multi-disciplinary open access archive for the deposit and dissemination of scientific research documents, whether they are published or not. The documents may come from teaching and research institutions in France or abroad, or from public or private research centers.

L'archive ouverte pluridisciplinaire **HAL**, est destinée au dépôt et à la diffusion de documents scientifiques de niveau recherche, publiés ou non, émanant des établissements d'enseignement et de recherche français ou étrangers, des laboratoires publics ou privés.

Accepted Manuscript

Title: The four cysteine residues in the second extracellular loop of the human adenosine A_{2B} receptor: role in ligand binding and receptor function

Authors: Anke C. Schiedel, Sonja Hinz, Dominik Thimm, Farag Sherbiny, Thomas Borrmann, Astrid Maaß, Christa E. Müller



PII: S0006-2952(11)00301-7
DOI: doi:10.1016/j.bcp.2011.05.008
Reference: BCP 10900

To appear in: *BCP*

Received date: 18-2-2011
Revised date: 9-5-2011
Accepted date: 11-5-2011

Please cite this article as: Schiedel AC, Hinz S, Thimm D, Sherbiny F, Borrmann T, Maaß A, Müller CE, The four cysteine residues in the second extracellular loop of the human adenosine A_{2B} receptor: role in ligand binding and receptor function, *Biochemical Pharmacology* (2010), doi:10.1016/j.bcp.2011.05.008

This is a PDF file of an unedited manuscript that has been accepted for publication. As a service to our customers we are providing this early version of the manuscript. The manuscript will undergo copyediting, typesetting, and review of the resulting proof before it is published in its final form. Please note that during the production process errors may be discovered which could affect the content, and all legal disclaimers that apply to the journal pertain.

1
2
3
4 **The four cysteine residues in the second extracellular loop of the human**
5
6 **adenosine A_{2B} receptor: role in ligand binding and receptor function**
7
8
9

10
11 Anke C. Schiedel^{a,*}, Sonja Hinz^a, Dominik Thimm^a, Farag Sherbiny^b, Thomas
12
13 Borrmann^a, Astrid Maaß^b, and Christa E. Müller^a
14
15
16
17

18
19 ^aPharmaCenter Bonn, Pharmaceutical Institute, Pharmaceutical Chemistry I, University
20
21 of Bonn, An der Immenburg 4, D-53121 Bonn, Germany
22

23
24 ^bFraunhofer Institute SCAI, Schloss Birlinghoven, 53754 Sankt Augustin, Germany
25

26 *corresponding author: schiedel@uni-bonn.de, phone ++49 (228) 736457; fax ++49
27
28 (228) 732567; An der Immenburg 4, D-53121 Bonn, Germany
29

30
31 shinz@uni-bonn.de, dthimm@uni-bonn.de, fselim@uni-bonn.de,

32
33 thomas.borrmann@uni-bonn.de , astrid.maass@scai.fraunhofer.de,

34
35
36 christa.mueller@uni-bonn.de
37
38
39

40
41 category: (5) Inflammation and Immunopharmacology
42
43
44
45
46
47
48
49
50
51
52
53
54
55
56
57
58
59
60
61
62
63
64
65

Abstract

The adenosine A_{2B} receptor is of considerable interest as a new drug target for the treatment of asthma, inflammatory diseases, pain, and cancer. In the present study we investigated the role of the cysteine residues in the extracellular loop 2 (ECL2) of the receptor, which is particularly cysteine-rich, by a combination of mutagenesis, molecular modeling, chemical and pharmacological experiments. Pretreatment of CHO cells recombinantly expressing the human A_{2B} receptor with dithiothreitol led to a 74-fold increase in the EC₅₀ value of the agonist NECA in cyclic AMP accumulation. In the C78^{3.25}S and the C171^{45.50}S mutants high-affinity binding of the A_{2B} antagonist radioligand [³H]PSB-603 was abolished and agonists were virtually inactive in cAMP assays. This indicates that the C3.25-C45.50 disulfide bond, which is highly conserved in GPCRs, is also important for binding and function of A_{2B} receptors. In contrast, the C166^{45.45}S and the C167^{45.46}S mutants as well as the C166^{45.45}S-C167^{45.46}S double mutant behaved like the wild-type receptor, while in the C154^{45.33}S mutant significant, although more subtle effects on cAMP accumulation were observed - decrease (BAY60-6583) or increase (NECA) - depending on the structure of the investigated agonist. In contrast to the X-ray structure of the closely related A_{2A} receptor, which showed four disulfide bonds, the present data indicate that in the A_{2B} receptor only the C3.25-C45.50 disulfide bond is essential for ligand binding and receptor activation. Thus, the cysteine residues in the ECL2 of the A_{2B} receptor not involved in stabilization of the receptor structure may have other functions.

Keywords

1
2
3
4
5
6
7 Adenosine A_{2B} receptor; disulfide bonds; extracellular loop 2; mutagenesis; PSB-603
8
9

10 11 **1 Introduction** 12 13 14

15
16 Adenosine A_{2B} receptors belong to the large group of purinergic G protein-coupled
17
18 receptors (GPCRs), which comprise P2 (P2Y and P2X, nucleotide-activated) and P1
19
20 (adenosine) receptors [1]. Brunschweiler and Müller [2] proposed to add P0 (adenine)
21
22 receptors as a third class to the group of purinergic receptors. The P1 or adenosine
23
24 receptor (AR) family consists of four subtypes, A₁, A_{2A}, A_{2B} and A₃ [3]. A₁ and A₃
25
26 receptors are coupled to G_i type G proteins, leading to the inhibition of the adenylate
27
28 cyclase upon receptor activation, while A_{2A} and A_{2B} receptors are mainly coupled to G_s
29
30 proteins resulting in an increase in intracellular cAMP concentrations via stimulation of
31
32 adenylate cyclase [4]. In several cell systems, such as HEK-293 and HMC-1 mast cells
33
34 A_{2B} receptors are additionally coupled to phospholipase C via G_q proteins, and are
35
36 thereby linked to intracellular Ca²⁺ release [5-6]. In the human leukemia cell line Jurkat
37
38 T, A_{2B}-mediated calcium mobilization independent of inositol-1,4,5-trisphosphate was
39
40 observed [7]. Coupling of the A_{2B} receptor to the MAPK cascade via ERK1/2 has been
41
42 described for recombinant CHO cells overexpressing human A_{2B} receptors and for mast
43
44 cells, showing an involvement in proliferation, differentiation and apoptosis [4, 8].
45
46 Furthermore a link of A_{2B} receptor signaling to the arachidonic acid signal transduction
47
48 pathway via phospholipase A and cyclooxygenase activation leading to vasoconstriction
49
50 in smooth muscle cells has been described [9].
51
52
53
54
55
56
57
58
59
60
61
62
63
64
65

1
2
3
4 Among the four AR subtypes A_{2B} has been the least well characterized receptor, mainly
5 due to the lack of suitable, specific ligands [10]. Meanwhile highly selective A_{2B}
6
7 antagonists have been developed and an A_{2B} -specific antagonist radioligand, [3H]PSB-
8
9 603 (for structure see figure 1), with high potency and specificity across species,
10 including rodents and humans, has recently become available [11]. As for agonists,
11 besides the nucleoside derivative NECA [12], which is non-selective, and related
12
13 adenosine derivatives, the first highly selective A_{2B} agonist BAY60-6583 [13], a non-
14
15 nucleosidic compound, has been developed (structures are shown in supplemental
16
17 figure 1).
18
19
20
21
22
23
24

25
26 In many tissues, A_{2B} receptors are considered low affinity receptors with typically low
27
28 expression levels [14]. Therefore, adenosine concentrations typically have to reach
29
30 micromolecular levels to activate natively expressed A_{2B} receptors, which occurs under
31
32 pathological conditions, such as hypoxia, ischemia, inflammation or massive cell death
33
34 [15-16]. While their distribution is ubiquitous, A_{2B} receptors are found at higher densities
35
36 mainly in the large intestine, in mast cells, hematopoietic cells, and in the brain, mainly
37
38 in astrocytes [6, 14, 17-18]. Upregulation has been found in several cancer cell lines
39
40 [19]. A_{2B} receptors are thought to be involved in a number of diseases and the first
41
42 antagonist is now being evaluated in clinical trials for the treatment of asthma and
43
44 chronic obstructive pulmonary disease [10]. Other potential indications include secretory
45
46 diarrhea associated with inflammation, Alzheimer's disease, inflammatory diseases,
47
48 pain, cancer, type II diabetes, and diabetic retinopathy [20]. Thus, A_{2B} receptors
49
50 represent important new drug targets.
51
52
53
54
55
56

57 To fully understand interactions of the human A_{2B} receptor with its ligands, agonists and
58
59 antagonists, it is of major importance to gain knowledge about the structure of the
60
61
62
63
64
65

1
2
3
4 receptor, the amino acid residues involved in ligand binding, and to determine the
5
6 receptor's 3D structure, which in turn can then be used for the development of new
7
8 ligands [21-22]. Except for a few mutagenesis studies [16, 23-25] and homology models
9
10 [26-28], the most recent one based on the X-ray structure of the closely related A_{2A}
11
12 receptor [29], not much structural information about the A_{2B} receptor is available.
13
14

15
16 A common feature of most GPCRs is the existence of a highly conserved disulfide bond
17
18 between C3.25 (Ballesteros Weinstein nomenclature [30]) at the extracellular site of
19
20 transmembrane domain 3 (TMD3) and cysteine residue C45.50 [31] in the extracellular
21
22 loop 2 (ECL2) located between TMD4 and TMD5 [26-27, 32]. Recently de Graaf et al.
23
24 [31] undertook a molecular modeling project and aligned ECL2 sequences of 365
25
26 human GPCRs. More than 92 % of the investigated receptors showed the conserved
27
28 disulfide bond.
29
30

31
32
33 The A_{2B} receptor possesses the longest ECL2 of all four adenosine receptor subtypes,
34
35 with four cysteine residues - the highest number found in any GPCR - of which three
36
37 (C154, C167, C171) are homologous to the three (C146, C159, C166) found in the A_{2A}
38
39 receptor (see figures 1 and 2). Those four cysteine residues are not conserved in the
40
41 known mammalian A_{2B} receptor orthologs. Therefore, the goal of the present study was
42
43 to investigate the role of the cysteine residues in the cysteine-rich ECL2 of the A_{2B}
44
45 receptor with respect to disulfide bond formation, ligand binding, and receptor activation.
46
47
48
49
50

51
52
53 *insert figure 1 here*
54
55
56

57 **2 Material and Methods**

58
59
60
61
62
63
64
65

1
2
3
4 All chemicals were obtained from Roth (Karlsruhe, Germany) or Applichem (Darmstadt,
5
6 Germany) unless otherwise noted. Radioligands were obtained from Quotient
7
8 Bioresearch (Cardiff, UK).
9

10 11 12 13 14 **2.1 Alignments of extracellular loops, prediction of disulfide bonds and loop** 15 16 **simulation** 17

18
19
20
21 Alignments of extracellular loops 1 and 2 of the human A_{2A} and A_{2B} receptors were
22
23 performed using Clustal W2 [33]. Similarity was determined using EMBOSS [34].
24
25 Prediction of N-glycosylation was done with NetNGlyc 1.0 from the CBS prediction
26
27 servers [35]. The topology was illustrated using TOPO2 [36]. Modeling of the non-
28
29 conserved part of the extracellular loop 2 of the adenosine A_{2B} receptor was performed
30
31 with the ModLoop modeling algorithm based on global optimization of conformational
32
33 energy [37]. In all models, residues in the transmembrane domains and the intracellular
34
35 loops were restrained by harmonic force to their reference position during simulation;
36
37 only residues of ECL1 and ECL2 were allowed to move. Loop conformations emerging
38
39 from this procedure were minimized stepwise with respect to the force field energy by
40
41 using the Amber package to obtain a low energy conformation [38]. Then the annealing
42
43 molecular dynamics (MD) was used to optimize the accommodation of ECL1 and ECL2,
44
45 where the loop atoms were heated from 100 K to 450 K and cooled to 100 K over a
46
47 period of 1.6 ns. The MD simulations were performed accordingly, restraints with a force
48
49 constant of 0.5 Kcal/mol.Å² were applied to TMDs for 400 ps: heated from 100 K to 450
50
51 K and 1.2 ns: then cooled from 450 K to 100 K. The time step of the simulations was 2.0
52
53 fs with a cutoff of 10 Å for the non-bonded interactions. The geometrical parameters of
54
55
56
57
58
59
60
61
62
63
64
65

1
2
3
4 the created models were evaluated and compared with the crystal structure of the A_{2A}
5
6 receptor using PROCHECK and PROSAIL [39-40].
7
8
9

10 11 **2.2 Cell culture**

12
13
14
15
16 GP+envAM12 packaging cells (ATCC CRL-9641) were cultured at 37 °C and 5 % CO₂
17
18 in Dulbecco's modified Eagle medium (DMEM; Invitrogen, Darmstadt, Germany),
19
20 containing 10% FCS, 100 U/ml penicillin G, 100 µg/ml streptomycin, 1% ultraglutamine,
21
22 200 µg/ml hygromycin B, 15 µg/ml hypoxanthine, 250 µg/ml xanthine and 25 µg/ml
23
24 mycophenolic acid. Chinese hamster ovary (CHO) cells were maintained in DMEM-F12
25
26 medium (Invitrogen, Darmstadt, Germany) with 10% FCS, 100 U/ml penicillin G, 100
27
28 µg/ml streptomycin and 1% ultraglutamine under the same conditions. All supplements
29
30 were from Invitrogen (Darmstadt, Germany), and antibiotics were from Calbiochem
31
32 (Merck, Darmstadt, Germany).
33
34
35
36
37
38
39

40 41 **2.3 Site-Directed Mutagenesis**

42
43
44
45 The coding sequence for the human adenosine A_{2B} receptor was cloned into the plasmid
46
47 vector pUC19. Point mutations leading to the desired amino acid exchanges were
48
49 introduced through site-directed mutagenesis using whole plasmid recombination PCR.
50
51 Complementary oligonucleotide primers were designed containing the corresponding
52
53 mutations. Therein, each mismatched base is flanked by 12-19 nucleotides at the 3' and
54
55 5' end of the primer. The PCR reaction mixture contained 20 ng of template DNA, 15
56
57 pmol of each primer, 10 mM dNTPs, 1 × Thermopol reaction buffer and 1 U Vent_R
58
59
60
61
62
63
64
65

1
2
3
4 polymerase (New England Biolabs, Frankfurt, Germany). The PCR was performed using
5
6 the following cycle program: 4 min at 94 °C, 20 cycles consisting of 1 min at 94 °C, 1
7
8 min at 66 °C, and 10 min at 72 °C followed by a final elongation step of 10 min at 72 °C.
9
10 The final PCR product was digested with the restriction enzyme *DpnI* (New England
11
12 Biolabs, Frankfurt, Germany) for 90 min to degrade any parental template DNA. After
13
14 transformation of competent *Escherichia coli* Top10 cells with the digested PCR product,
15
16 plasmids from single colonies were isolated and sequenced (GATC Biotech, Konstanz,
17
18 Germany). Mutated receptor DNAs were subsequently subcloned into the retroviral
19
20 plasmid vector pLXSN, which contained a hemagglutinin (HA) tag, resulting in an N-
21
22 terminally tagged receptor after translation. Transformation, isolation and sequencing of
23
24 the newly constructed plasmid were performed.
25
26
27
28
29
30
31
32

33 **2.4 Retroviral transfection and membrane preparation**

34
35
36
37

38 CHO cells were stably transfected using a retroviral transfection system as described
39
40 before [11]. After one week the G418 concentration which is used for the selection was
41
42 reduced to 200 µg/ml. For membrane preparations several dishes of stably transfected
43
44 CHO cells were grown to confluence, and then cells were washed and scraped off using
45
46 50 mM Tris-HCl, pH 7.4, containing 2 mM EDTA. After homogenization the cell
47
48 suspension was centrifuged for 10 min at 1000 x g and 4 °C. The low speed supernatant
49
50 was then centrifuged at 48,000 x g and 4 °C for 1 h. Membrane pellets were
51
52 resuspended in 50 mM Tris-HCl, pH 7.4, and centrifugation was repeated under the
53
54 same conditions. Membranes were aliquoted and stored at -80 °C until further use. The
55
56
57
58
59
60
61
62
63
64
65

1
2
3
4 protein concentration of the membrane preparation was determined using the method
5
6 described by Lowry et al. [41].
7
8
9

10 11 **2.5 Cell Surface ELISA** 12 13

14
15
16 The cell surface expression of wt and mutant receptors, stably expressed in CHO cells
17
18 was determined using ELISA as previously described [42]. In brief, cells were seeded
19
20 into 24 well plates 24 h before the assay. Cells were washed with PBS and blocked for 5
21
22 min with PBS/1 % BSA. HA antibody (Covance, Munich, Germany) was diluted 1:1000
23
24 in DMEM, 1 % BSA, 10 mM HEPES, pH 7.0, 1 mM CaCl₂ and added to the cells for 1 h at
25
26 room temperature. After washing (3 x PBS, 5 min each) cells were fixed with 4 %
27
28 paraformaldehyde in PBS, washed again and blocked for 10 min. The peroxidase-
29
30 coupled secondary antibody (goat anti mouse, Sigma, Munich, Germany) was diluted
31
32 1:2500 in PBS/1 % BSA and added to the cells for 1 h at room temperature, after which
33
34 cells were washed again 4 x with PBS. 300 µl prewarmed ABTS substrate (Thermo
35
36 scientific Pierce, Rockford, USA) was added and cells were incubated for 50 min. 170 µl
37
38 of the substrate were transferred to 96-well plates and absorption was measured at 405
39
40 nm using fresh substrate as a reference. Experiments were performed in two to six
41
42 independent experiments, each in triplicates.
43
44
45
46
47
48
49
50
51
52

53 **2.6 Radioligand Binding Experiments** 54 55 56

57
58 Competition experiments were performed using the high affinity antagonist radioligand
59
60 [³H]PSB-603 [11]. The wild-type receptor (wt) and the mutants C78S, C166S, C167S,
61
62
63
64
65

1
2
3
4 and C171S were analyzed in a final volume of 500 μ l. The vials contained 25 μ l of the
5
6 test compound dissolved in 50% DMSO / 50% Tris-HCl (50 mM, pH 7.4), 275 μ l of 50
7
8 mM Tris-HCl buffer (pH 7.4), 100 μ l of radioligand solution in the same buffer (final
9
10 concentration 0.3 nM), and 30 μ g of membrane preparations (diluted in 100 μ l Tris-HCl,
11
12 pH 7.4) which had been preincubated with ADA (2 U/ml) for 20 min. The mutants C154S
13
14 and C166S-C167S were analyzed in radioligand binding assays in a final volume of 200
15
16 μ l containing 50 μ l of test compound diluted in 10% DMSO / 90% Tris-HCl (50 mM, pH
17
18 7.4), 50 μ l radioligand diluted in Tris-HCl buffer (50 mM, pH 7.4, final concentration of
19
20 the radioligand 0.3 nM) and 50 μ g of membrane preparations, diluted in 100 μ l buffer,
21
22 pretreated with ADA (2 U/ml) 20 min before use. Total binding was determined in the
23
24 absence of test compound; nonspecific binding was measured in the presence of 10 μ M
25
26 8-cyclopentyl-1,3-dipropylxanthine (DPCPX). After 75 min at room temperature samples
27
28 were harvested by filtration through GF/B glass fiber filters. Filters were washed with ice-
29
30 cold buffer containing 50 mM Tris-HCl (pH 7.4) and 0.1% bovine serum albumin (BSA),
31
32 and subsequently transferred into scintillation vials. The liquid scintillation counting of
33
34 the filters started after 9 h of pre-incubation in 2.5 ml of scintillation cocktail (Lumag AG,
35
36 Basel) in order to allow the radioligand to diffuse into the scintillation cocktail. Three
37
38 independent experiments were performed each in triplicates. If the sample volume for
39
40 incubation was reduced to 200 μ l depletion occurred due to the high affinity and low
41
42 concentration of the radioligand [3 H]PSB-603, which means that the free ligand
43
44 concentration in the solution was actually lower than the concentration added [43].
45
46
47
48
49
50
51
52
53
54
55
56

57 **2.7 Saturation assays**

58
59
60
61
62
63
64
65

1
2
3
4 Saturation experiments were performed in duplicates as described in paragraph 2.6 with
5 radioligand concentrations ranging from 0.05 - 1.6 nM in 50 mM Tris-HCl (pH 7.4).
6
7
8
9

10 11 **2.8 Determination of intracellular cAMP accumulation**

12
13
14

15
16 Stably transfected CHO cells expressing the wild-type or mutant receptors were plated
17 onto 24 well plates at a density of 200,000 cells per well. After 24 h the medium was
18 removed and the cells were washed with 500 μ l of 37 °C warm Hank's Balanced Salt
19 Solution (HBSS; 20 mM HEPES, 135 mM NaCl, 5.5 mM glucose, 5.4 mM KCl, 4.2 mM
20 NaHCO₃, 1.25 mM CaCl₂, 1 mM MgCl₂, 0.8 mM MgSO₄, 0.44 mM KH₂PO₄ and 0.34 mM
21 Na₂HPO₄, pH adjusted to 7.3) containing 1 U/ml of adenosine deaminase (ADA, Sigma).
22
23 The cells were then incubated in 300 μ l of HBSS with ADA at 37 °C and 5 % CO₂ for 2
24 h. Then, 100 μ l of the phosphodiesterase inhibitor Ro20-1724 (Hoffmann La Roche,
25 Grenzach, Germany; final concentration 40 μ M) were added to each well and the cells
26 were incubated for 15 min at 37 °C and 5% CO₂. Then 100 μ l of various dilutions of the
27 agonists 5'-N-ethylcarboxamidoadenosine (NECA; Sigma, Munich, Germany), or
28 BAY60-6583 (Bayer Schering Pharma), respectively in HBSS containing 5 % DMSO
29 were added in triplicates (final DMSO concentration 0.5%). After 15 min of incubation at
30 37 °C and 5% CO₂ the supernatant was removed and 500 μ l of 90 °C hot lysis buffer
31 consisting of 4 mM EDTA and 0.01% Triton X-100 with the pH adjusted to 7.3 were
32 added. After one hour of mixing on ice, cAMP amounts of the lysates were determined
33 by competitive radioligand binding experiments [44]. Competition experiments were
34 performed in a final volume of 120 μ l containing 50 μ l of cell lysates, 30 μ l of [³H]cAMP
35 radioligand solution in lysis buffer (final concentration 3 nM) and 40 μ l of cAMP binding
36
37
38
39
40
41
42
43
44
45
46
47
48
49
50
51
52
53
54
55
56
57
58
59
60
61
62
63
64
65

1
2
3
4 protein [44] diluted in the same buffer (50 µg per sample). For determining cAMP
5
6 concentrations 50 µl of various cAMP concentrations were measured instead of cell
7
8 lysates, to obtain a standard curve. Total binding was determined by adding radioligand
9
10 and binding protein to lysis buffer, and the background was determined without addition
11
12 of binding protein. The mixture was incubated for 60 min on ice and filtered through a
13
14 GF/B glass fiber filter using a cell harvester (Brandel, Unterföhring, Germany). The filters
15
16 were washed three times with 2-3 ml of ice-cold 50 mM Tris-HCl buffer, pH 7.4 and
17
18 subsequently transferred into scintillation vials. The liquid scintillation counting of the
19
20 filters started after 9 h of incubation in 2.5 ml of scintillation cocktail (Lumag AG, Basel).
21
22 Three separate experiments were performed. The amount of cAMP was determined by
23
24 comparison to a standard curve generated for each experiment and plotted as percent
25
26 of maximal NECA stimulation.
27
28
29
30
31
32
33
34
35

36 **2.9 Experiments with DTT pretreatment**

37
38
39

40 The effect of dithiothreitol (DTT) on receptor function was investigated by measuring
41
42 NECA-induced cAMP accumulation as described in 2.8, except that CHO cells, stably
43
44 expressing the human A_{2B} receptor, were preincubated with 10 mM DTT for 2 h at 37°C.
45
46
47
48
49

50 **3 Results**

51
52
53
54

55 **3.1 Comparison of extracellular loops 1 and 2 of A_{2A} and A_{2B} receptors**

56
57
58
59
60
61
62
63
64
65

1
2
3
4 The A_{2A} receptor is the adenosine receptor subtype, which is most closely related to the
5
6 A_{2B} receptor. Sequence analysis of the human A_{2A} and A_{2B} receptors show an overall
7
8 identity of 58 % and a similarity of 73 %. The most conserved residues are found within
9
10 the transmembrane domains. By comparing the extracellular loops 1 and 2, which show
11
12 44 % and 34 % identity, and 56 % and 46 % similarity, respectively, one can find
13
14 extremely high degrees of homology when comparing the residues close to the cysteine
15
16 residues C71, C77, C166 in the A_{2A} receptor and the corresponding residues C72, C78,
17
18 C171 in the A_{2B} receptor (see figure 2). The residues adjacent to those cysteine
19
20 residues are identical or at least similar in A_{2A} and A_{2B} receptors in both extracellular
21
22 loops. The region between the conserved cysteine C45.50 (C166 in A_{2A}, C171 in A_{2B}) in
23
24 ECL2 and TMD5 is even 86 % identical and 100 % similar, providing evolutionary
25
26 evidence for the importance of that partial structure. The ECL2 of both receptors contain
27
28 potential N-glycosylation sites between the highly similar stretch between the conserved
29
30 cysteine residues C146 and C159 in the A_{2A} receptor, and C154 and C167 in the A_{2B}
31
32 receptor, respectively. The A_{2B} receptor contains a second potential N-glycosylation site
33
34 at N153, where C154 is part of the sequon. The A_{2B} receptor has a 7-amino acid
35
36 insertion at the site close to TMD4 and a 3-amino acid gap between the conserved
37
38 cysteine residues C167 and C171, moving those cysteine residues and the adjacent
39
40 glycosylation site closer together as compared to the A_{2A} receptor. The crystal structure
41
42 of the A_{2A} receptor [45] shows two β -sheets in ECL1 and ECL2 both being in an
43
44 antiparallel conformation. According to the refined computer model based on the
45
46 published model [29], the A_{2B} receptor can also form one β -sheet in each of the
47
48 extracellular loops 1 and 2, which appear to be close enough together to be able to form
49
50
51
52
53
54
55
56
57
58
59
60
61
62
63
64
65

1
2
3
4 antiparallel sheets. Despite similarities between the adenosine A_{2A} and the A_{2B} receptor
5
6 subtypes with regard to the cysteine residues localized close to or in the extracellular
7
8 part of the proteins there are significant differences, and their roles and functions may
9
10 be different.
11
12

13
14
15
16 *insert figure 2 here*
17
18
19
20

21 **3.2 Disulfide bond prediction**

22
23
24
25
26 For predicting disulfide bonds in the ECL2 of the A_{2B} receptor, models of the A_{2A}
27
28 receptor based on the published X-ray structure were initially generated for testing the
29
30 procedure. One of the generated models (m1 A_{2A}) contained the highly conserved
31
32 disulfide bond between C3.25 and C45.50, corresponding to C77 (TMD3) and C166
33
34 (ECL2), while a second model (m2 A_{2A}) contained all four possible bonds (C77-C166,
35
36 C74-C146, C71-C159, and C259-C262), which were observed in the X-ray structure of
37
38 the A_{2A} receptor [45]. Table 1 lists the fixed disulfide bonds and the results of the
39
40 analyses used to evaluate the goodness of the models obtained by several programs,
41
42 such as PROCHECK (Psi/Phi angles), PROSAIL (Z-scores) and root mean square
43
44 distances (RMSD), both in comparison to the A_{2A} X-ray structure and the initial A_{2A} or
45
46 A_{2B} model. The psi/phi angles, which are obtained by PROCHECK are determined using
47
48 a Ramachandran plot, which is a way to visualize the dihedral angles (psi against phi) of
49
50 amino acid residues in protein structures, where psi is the angle between carbon and
51
52 carbonyl and phi the angle between carbon and nitrogen. Lower values indicate better
53
54 quality of the model. Z-scores, obtained by PROSAIL, indicate the overall model quality;
55
56
57
58
59
60
61
62
63
64
65

1
2
3
4 its value is displayed in a plot which shows the local model quality by plotting energies
5
6 as a function of the amino acid sequence position. In general, positive values
7
8 correspond to problematic parts of the input structure, negative values indicate good
9
10 quality. RMSD values are a useful way to compare two models either of the same
11
12 structure or two closely related structures, such as the crystal structure of the A_{2A}
13
14 receptor and the model of the the A_{2B} receptor. The values reflect the average distances
15
16 between the backbones of the proteins. Lower values indicate good accordance
17
18 between two models or structures. Model 2, containing all four disulfide bonds, observed
19
20 in the A_{2A} crystal structure (m2 A_{2A}) led to better values and scores and was therefore
21
22 chosen as reference for the predictions of disulfide bonds in the A_{2B} receptor (see table
23
24 1). Four different A_{2B} receptor models with combinations of fixed disulfide bonds were
25
26 compared to m2 A_{2A} and the initial A_{2B} model without any disulfide bonds [29]. Figure 3A
27
28 shows the positions of the cysteine residues potentially involved in disulfide bond
29
30 formation in the initial A_{2B} model before loop simulation, as well as the two asparagine
31
32 residues, which could be glycosylated. According to the Z-score, model 2 (m2 A_{2B})
33
34 containing two disulfide bonds, C78-C171 and C72-C167, would be the preferred model,
35
36 since positive values correspond to problematic parts of the input structure while
37
38 negative values indicate high quality. According to all other parameters determined,
39
40 model 1 (m1 A_{2B}), containing only the highly conserved disulfide bond between TMD3
41
42 and ECL2, C78-C171, is the most likely prediction. The more significant analysis of the
43
44 loop motions during simulation allows a comparison of the fluctuation profiles along the
45
46 sequences of all models (see figure 4). Since all protein parts except for ECL1 and
47
48 ECL2 have been restrained to their initial position during simulation, only motions in the
49
50 ECL1 and ECL2 segments are observed. It was found that m1 A_{2B} and m4 A_{2B} , i.e. the
51
52
53
54
55
56
57
58
59
60
61
62
63
64
65

1
2
3
4 model with the lowest number of disulfide bonds and the one with the highest number of
5
6 disulfide bonds, produce B-factor profiles very similar to the one of the tightly
7
8 constrained m2 A_{2A} model with four disulfide bonds. B-factors indicate the true static or
9
10 dynamic mobility of an atom; it can also indicate errors in model building (reflected in
11
12 higher values, corresponding to the peaks in figure 4). However, introducing a disulfide
13
14 bond between C72-C166 and C72-C167, respectively, apparently leads to a structural
15
16 destabilization. The analysis of average B-factors shows a preference for models 1 and
17
18 4 (see figure 4). ECL2 contains two potential glycosylation sites, N153 and N163, both
19
20 close to cysteine residues. In model 1 and model 2 both sites are accessible for
21
22 glycosylation. As shown in figure 3B, in model 1 the two extracellular loops 1 and 2 are
23
24 held together by two antiparallel β -sheets, while the loops in model 2 are connected by a
25
26 second disulfide bond between C72 and C167. The β -sheet in ECL1 appears to be very
27
28 stable, while the β -sheet in ECL2 was less stable during the simulation process. With the
29
30 β -sheet present in ECL2, C72 and C167 are about 10 Å apart, making it very unlikely to
31
32 form a disulfide bond. Model 3, having a second disulfide bond between C72 and C166,
33
34 is less likely than models 1 and 2 according to the values and scores (see table 1), and
35
36 model 4 can be excluded because of unfavorable values (see table 1), in addition, both
37
38 potential glycosylation sites are not exposed to the solvent, but are facing the helices.
39
40 Thus, molecular modeling studies indicate that the A_{2B} receptor might contain a second
41
42 disulfide bond (C72-C167) next to the highly conserved bond between C78 and C171
43
44 (model 2).
45
46
47
48
49
50
51
52
53
54
55
56
57

58 ***insert figures 3 and 4, and table 1 here***
59
60
61
62
63
64
65

3.3. Effects of DTT pretreatment on A_{2B} receptor activity

A first experimental indication that disulfide bond formation is essential for A_{2B} receptor function was obtained by preincubating CHO cells stably expressing human A_{2B} receptors with DTT followed by NECA-induced cAMP accumulation assays. As shown in figure 5 the curve for the agonist NECA was shifted to the right by 74-fold compared to A_{2B} receptor activity without DTT pretreatment (EC₅₀ values: 2720 nM vs. 36.6 nM).

insert figure 5 here

3.4 Comparison of A_{2B} wild-type receptors with and without HA tag

As a next step we planned to exchange each of the cysteine residues in ECL2 of the human A_{2B} receptor for serine. For comparison of the mutant receptors with the wild-type receptor it was essential to determine their cell surface expression by ELISA. Therefore tagging of the receptors was required. Receptors were HA-tagged at the N terminus, which had been shown not to interfere with ligand binding and function for several other GPCRs [42]. Potential interference of the tag at the A_{2B}AR was investigated in radioligand binding as well as in functional assays. As shown in figure 6 binding of ligands to the HA-tagged A_{2B} receptor was not altered in comparison to the wt receptor. K_D values (untagged wt: 0.403 ± 0.188 nM, HA-tagged wt: 0.473 ± 0.170 nM) calculated from saturation experiments were not significantly different (see figure 7). Although B_{max} values (untagged wt: 502 ± 57 fmol/mg, HA-tagged wt: 283 ± 37 fmol/mg)

1
2
3
4 differed slightly, expression of both, tagged and untagged receptors was in the same
5
6 range. Neither for the antagonist PSB-603 nor for the agonists NECA and BAY60-6583
7
8 significant differences of K_i values determined in radioligand binding studies could be
9
10 found (see supplemental table 1 and figure 6). When comparing the functionality of the
11
12 HA-tagged receptors to the wild-type receptors no significant differences could be
13
14 detected either. Figure 8 shows the results of cAMP accumulation experiments using
15
16 whole cells with two structurally different agonists, NECA (figure 8A) and BAY60-6583
17
18 (figure 8B and supplemental table 1). For NECA, EC_{50} values of 26.9 ± 4.5 nM
19
20 (untagged) and 36.6 ± 4.8 nM (tagged) were determined, and for BAY60-6583 $37.5 \pm$
21
22 12.3 nM and 42.4 ± 4.4 nM, respectively.
23
24
25
26
27
28
29
30

31 *insert figures 6-8 here*

32 33 34 35 36 **3.5 Characterization of mutant receptors**

37
38
39
40 All receptor cDNA sequences were subcloned into the retroviral expression vector
41
42 pLXSN and stably expressing CHO cells were generated. Cysteine residues (C78,
43
44 C154, C166, C167, and C171) which were replaced by serine via site directed
45
46 mutagenesis are highlighted in a topology model of the A_{2B} receptor (figure 1). Cell
47
48 surface expression levels for all mutants were determined by ELISA and compared to
49
50 that of the wt receptor (see figure 9)
51
52
53
54
55
56

57 *insert figure 9 here*

1
2
3
4 Cysteine mutants were analyzed in radioligand binding studies using the antagonist
5 radioligand [³H]PSB-603 versus unlabeled PSB-603 as well as versus the agonist NECA
6
7 (see supplemental figure 2). All mutants were compared to the wt receptor. Binding of
8
9 [³H]PSB-603 (0.3 nM) to C78S and C171S mutants was completely abolished; therefore
10
11 no competition binding curves could be determined. In contrast, the mutants C166S,
12
13 C167S, and the double mutant C166S-C167S showed similar affinity for PSB-603 and
14
15 NECA as the wt receptor. A difference was, however, seen with C154S: it exhibited a
16
17 significantly, 8-fold increased IC₅₀ value for PSB-603, while no significant difference was
18
19 observed for the agonist NECA (table 2).
20
21
22
23
24
25
26
27

28 ***insert table 2 here***
29
30
31
32

33 NECA-induced cAMP accumulation was examined using cells expressing the generated
34
35 mutants (figure 10A). In contrast to the mutants C166S, C167S, and C166S-C167S,
36
37 which showed EC₅₀ values that were not significantly different from that determined at
38
39 the wt, the mutants C78S, C154S, and C171S showed significantly increased EC₅₀
40
41 values compared to the wild-type receptor (table 3). While the EC₅₀ value for the mutant
42
43 C154S was moderately (2.7-fold) increased, the dose-response curves for the mutants
44
45 C78S and C171S were dramatically shifted to the right, resulting in an almost 7000-fold
46
47 increase in the EC₅₀ value in the mutant C78S (397 000 ± 7 700 nM) compared to that of
48
49 the wild-type receptor (58.1 ± 1.2 nM), and a similarly large increase for the mutant
50
51 C171S (to 256 000 ± 28 900 nM). At the mutated receptors C78S and C171S the EC₅₀
52
53 of the non-nucleosidic agonist BAY60-6583 was also dramatically increased, similarly as
54
55 observed for NECA. Due to the limited solubility of BAY60-6583 full concentration-
56
57
58
59
60
61
62
63
64
65

1
2
3
4 response curves could, however, not be determined. In the other cysteine mutants
5
6 C154S, C166S, and C167S BAY60-6583 showed slightly decreased EC₅₀ values (only
7
8 ca. 2-fold; see figure 10B and table 3).
9

10
11
12
13
14 *insert figure 10 and table 3 here*
15

16 17 18 **4 Discussion** 19

20
21
22
23 The extracellular loops ECL1 [25], ECL2 [31], and ECL3 [42] of GPCRs belonging to the
24
25 rhodopsin family have been found to contribute considerably to receptor function [46].
26
27 However, extracellular loops differ widely in length, sequence, and structure between
28
29 different GPCRs and even between closely related receptor subtypes [31]. Cysteine
30
31 residues and disulfide bonds present in the extracellular domains of GPCRs have been
32
33 reported to play important roles in ligand binding, receptor stability, and receptor function
34
35 [32, 47-48]. The adenosine A_{2B} receptor contains the highest number of cysteine
36
37 residues in the ECL2 of all mammalian GPCRs (C154, C166, C167, C171) [31].
38
39 Therefore we were interested in studying the role of these cysteine residues and their
40
41 potential involvement in the formation of disulfide bonds.
42
43 Most rhodopsin-like GPCRs contain a disulfide bond between the highly conserved
44
45 cysteine residue C3.25 corresponding to C78 in the A_{2B} receptor, which is located in
46
47 TMD3 and the conserved cysteine residue C45.50 in the second extracellular loop
48
49 (C171 in A_{2B}). For several GPCRs this disulfide bond has been shown to play a critical
50
51 role for correct receptor conformation and activation [47]. The ECL2 is especially known
52
53 to be involved in antagonist binding, which could experimentally be shown for several
54
55
56
57
58
59
60
61
62
63
64
65

1
2
3
4 receptors, e.g. the dopamine D2 receptor [49] and the adenosine A₃ receptor [50].

5
6 Compared to the ECL2 of the other adenosine receptor subtypes, the ECL2 of the A_{2B}
7
8 receptor shows several differences: (i) the loop is between 4 and 10 amino acids longer;
9
10 (ii) ECL2 contains the most cysteine residues, four compared to three in A_{2A}, all of which
11
12 are involved in disulfide bonds according to the A_{2A} receptor crystal structure [45], and
13
14 only one in A₁ and A₃ receptors; (iii) the loop has two potential N-glycosylation sites
15
16 compared to only one in each of the other adenosine receptor subtypes. The highest
17
18 conservation of the ECL2 is found in the part of ECL2 which is close to TMD5. The
19
20 sequence upstream of the conserved cysteine is shorter than the corresponding
21
22 sequence in bovine rhodopsin, 9 amino acids compared to 14 amino acids [31]. The
23
24 conserved area between C45.50 and TMD5 is also very close to the binding pocket and
25
26 stabilized by the essential disulfide bond between TMD3 and ECL2, and therefore
27
28 probably not very flexible, while the less conserved area closer to TMD4 is highly flexible
29
30 and might be involved in ligand selection, or function as a cap in analogy to the gated
31
32 entrance pores described for several GPCRs [31, 51]. The β -sheet just upstream of the
33
34 conserved disulfide bond further stabilizes this end of ECL2. In the X-ray structure of the
35
36 A_{2A} receptor a second disulfide bond is holding the β -sheet in place making this area
37
38 even less flexible. This part of the loop could therefore be at least partly responsible for
39
40 the high affinity of the A_{2A} receptor for adenosine and related agonists by stabilizing the
41
42 active conformation. The loop in the A_{2A} receptor is shorter, and thus, the entrance to the
43
44 binding pocket is probably open and more accessible to the ligands. This hypothesis
45
46 may also explain why A_{2B} receptors typically show lower affinity for adenosine and
47
48 adenosine derivatives (agonists) than A_{2A} receptors, since the longer ECL2 of the A_{2B}
49
50
51
52
53
54
55
56
57
58
59
60
61
62
63
64
65

1
2
3
4 receptors may in some cases partially block the entrance to the binding pocket. The
5
6 ECL2 might be involved in transient, low-affinity ligand binding. Especially binding of
7
8 large ligands with long substituents extending to the receptor surface may interfere with
9
10 ECL2 movement or "gate closing". This might explain the effect of the C154S mutant on
11
12 PSB-603 binding. ECL2 movement may also be required for proper receptor activation.
13
14
15 In accordance with this hypothesis is the finding of Bokoch et al. describing ligand-
16
17 induced conformational changes of the extracellular surface of the β_2 adrenergic
18
19 receptor (β_2 AR), especially involving ECL2 and ECL3 [51]. They also describe the
20
21 formation of a structured cap which covers the opening of the binding pocket once a
22
23 ligand is bound, involving ECL2 and a salt bridge between an aspartate residue and a
24
25 lysine residue connecting ECL2 and ECL3. The A_{2B} receptor exhibits those amino acids
26
27 in equivalent positions (K269 at the transition from ECL3 to TMD7 corresponding to
28
29 Lys305 in the β_2 AR and Asp159 in ECL2 corresponding to Asp192 in the β_2 AR,
30
31 rendering a similar mechanism probable [51].
32
33
34
35
36
37
38
39
40

41 Dithiothreitol (DTT), a disulfide-reducing agent, which is commonly used to investigate
42
43 the importance of disulfide bonds in proteins, was applied to examine whether the A_{2B}
44
45 receptor possesses essential disulfide bonds necessary for receptor function [42]. As
46
47 shown in figure 5 a dramatic decrease in receptor function could be observed which has
48
49 also been shown for some other GPCRs containing the conserved disulfide bond
50
51 connecting TMD3 and ECL2 [42, 45]. These results clearly show that at least one
52
53 disulfide bond, susceptible to DTT reduction and, thus, presumably exposed to the
54
55 surface of the cell membrane, is important for receptor function.
56
57
58
59
60
61
62
63
64
65

1
2
3
4
5
6
7 Subsequently each cysteine residue of the A_{2B} receptor located in the ECL2, as well as
8
9 C78 in the external half of TMD3 was individually replaced by the sterically and
10
11 electronically similar serine, which lacks the ability to participate in disulfide bond
12
13 formation but is still able to form H-bonds, which are even stronger for the OH group of
14
15 serine than for the original SH group of its cysteine homologue. Through site-directed
16
17 mutagenesis DNA constructs coding for the mutations C78S (TMD3), C154S, C166S,
18
19 C167S, and C171S (ECL2) of the A_{2B} receptor were generated. In addition, a C166S-
20
21 C167S double mutant was constructed. To obtain comparable EC₅₀ values mutants
22
23 were compared to cells overexpressing wild-type receptors at the same level. Therefore
24
25 shifts of EC₅₀ values were due to reduced binding or function and not due to different
26
27 expression levels. Only two mutants, C78S and C171S showed somewhat lower
28
29 expression levels.
30
31
32
33
34
35
36
37

38 As predicted by the A_{2B} model it could clearly be shown, that C78 in TMD3 and C171 in
39
40 ECL2 are forming an important disulfide bond. The results obtained in radioligand
41
42 binding as well as functional studies showed a dramatic decrease in IC₅₀ and EC₅₀
43
44 values of several thousand-fold for the mutants C78S and C171S. All other mutants
45
46 either showed no difference or only moderate changes compared to the wild-type
47
48 receptor. It is known that disulfide bonds are already formed in the endoplasmic
49
50 reticulum (ER) and are very often necessary for proper folding and transport to the Golgi
51
52 apparatus. Therefore mutants without essential disulfide bonds are more prone to
53
54 degradation than wild-type receptors, further explaining somewhat lower cell surface
55
56 expression levels [47, 52]. While EC₅₀ values determined in functional studies may be
57
58
59
60
61
62
63
64
65

1
2
3
4 dependent on the receptor expression level, affinities measured in radioligand binding
5
6 studies are not. The extreme rightward shift of the concentration response curves in
7
8 functional assays can also not be explained by the somewhat lower expression levels in
9
10 the mutant receptors, which would be expected to cause only a moderate shift at the
11
12 most [42]. Thus it can be concluded that the disulfide bond C78-C171 in A_{2B} receptors is
13
14 essential for ligand binding and receptor function.
15
16
17
18
19
20

21 Based on the results of radioligand binding and functional assays as well as loop
22
23 simulations (figures 4, 9, 10; tables 1-3), model m1 A_{2B}, containing only the conserved
24
25 disulfide bond between C78 and C171, represents the most likely structure. It was
26
27 shown that this disulfide bond is essential for proper receptor function (figure 10).
28
29 According to our experimental data, all other disulfide bonds that had been predicted or
30
31 might be formed are less likely. If C72, located in the first extracellular loop, was
32
33 involved in linking ECL1 and ECL2 via a disulfide bond, similar to the situation found in
34
35 the A_{2A} X-ray structure [45], and this bond was essential for receptor function, one of the
36
37 ECL2 cysteine mutants should show different properties than the wild-type receptor.
38
39 ECL1 and ECL2 are held together by antiparallel β -sheets as predicted by the model m1
40
41 A_{2B}. Both β -sheets are also present in the A_{2A} receptor [45]. Two of the possible cysteine
42
43 residues proposed to be involved in forming a hypothetical second disulfide bond with
44
45 C72, namely C166 and C167 (m2 A_{2B} and m3 A_{2B}), are located adjacent to the putative
46
47 N-glycosylation site N163. Disulfide bond formation usually prevents glycosylation of
48
49 nearby glycosylation sites. When a disulfide bond cannot be formed due to mutagenesis
50
51 of cysteine residues, substitution of normally unused glycosylation sites is common [53].
52
53
54
55
56
57
58
59
60
61
62
63
64
65

1
2
3
4 In case C166 or C167 would be involved in a second disulfide bond with C72, N163
5
6 could be glycosylated in the cysteine mutants C166S, C167S, and C166S-C167S. This
7
8 glycosylation might then change the conformation of the receptor leading to larger
9
10 amounts of misfolded protein and to more degradation and, as a consequence, to lower
11
12 levels of cell surface expression, which was, however, not observed in our mutants (see
13
14 figure 9). Alternatively, N163-glycosylation could result in changes in ligand binding
15
16 and/or to altered function of the mutant receptors. However, in both mutants, C166S and
17
18 C167S as well as in the double mutant C166S-C167S neither changes in expression nor
19
20 binding and receptor function could be observed. This leads to the conclusion that both,
21
22 disulfide bond formation as well as glycosylation is unlikely. A further candidate cysteine
23
24 residue potentially involved in forming a hypothetical second bond with C72 is C154.
25
26 This amino acid residue is the central part of the sequon N-X-S/T for the putative N-
27
28 glycosylation site N153. If the bond were essential, an effect of the C154S in ligand
29
30 binding and receptor function were to be expected. If the bond is not formed,
31
32 glycosylation of N153 would be likely and should not be affected by the cysteine to
33
34 serine exchange, since the sequon N-X-S/T allows any amino acid except for proline in
35
36 the middle position. Thus, no change in ligand binding and receptor function should be
37
38 expected in the mutant if no disulfide bond is formed. Interestingly, A_{2B} receptors from
39
40 birds and bony fish, which only possess two cysteine residues in the ECL2 show the
41
42 closely related serine residue at that position. From the evolutionary point of view they
43
44 have developed independently from the mammalian A_{2B} receptors because they
45
46 separated even before the A_{2A} receptors emerged [54]. The A_{2A} receptor possesses an
47
48 asparagine residue adjacent to the cysteine residue corresponding to C154, but the
49
50 sequon is lost, probably in favor for gaining more stability of the loops through disulfide
51
52
53
54
55
56
57
58
59
60
61
62
63
64
65

1
2
3
4 bonds. Curiously, the mutant C154S showed an 8-fold decrease in affinity for the
5
6 antagonist PSB-603, while agonist binding was not significantly altered as compared to
7
8 the wild-type (supplemental figure 2, table 2). Receptor function of the C154S mutant on
9
10 the other hand was significantly altered depending on the agonist used. The nucleosidic
11
12 agonist NECA was about three-fold less potent, while the non-nucleosidic agonist
13
14 BAY60-6583 was slightly more potent at the C154S mutant receptor in comparison with
15
16 the wild-type receptor.
17
18
19

20
21 This leads to the hypothesis that free cysteine residues, especially C154, could play a
22
23 role in the interaction with specific ligands as it has been described for other GPCRs,
24
25 e.g. for P2Y₁₂ [48], the β 2 adrenergic receptor [55], or the cannabinoid receptor 2 [56].
26
27 Thus, free cysteine residues in the extracellular loops of the A_{2B} receptor may allow for
28
29 the development of new drugs, especially for inhibiting receptor function.
30
31
32

33
34
35 A possible explanation for the occurrence of the high number of cysteine residues in the
36
37 ECL2 of the A_{2B} receptor, which are not involved in disulfide bond formation under native
38
39 conditions, could be that they are part of a regulatory system, which may, for example,
40
41 explain the down-regulation of A_{2B} receptors during oxidative stress. Such an effect has
42
43 been described for alveolar macrophages from patients with chronic obstructive
44
45 pulmonary disease [57]. Oxidative stress leads to more oxidizing conditions in the ER
46
47 lumen, which in turn may lead to disulfide bond formation of non-native bonds, resulting
48
49 in more misfolded proteins, more degradation and finally to less A_{2B} receptors at the cell
50
51 surface. The A_{2A} receptor, which is upregulated under oxidative stress [45, 57] would not
52
53 be affected, because all four possible disulfide bonds are formed in the functional A_{2A}
54
55
56
57
58
59
60
61
62
63
64
65

1
2
3
4 receptor, at least according to the X-ray structure [45], as well as according to a recent
5
6 molecular modeling study [58].
7
8
9

10
11 The cysteine residues could be involved in controlling/regulating receptor function by
12
13 forming so-called allosteric disulfide bonds, e.g. by promoting or stabilizing the active or
14
15 inactive receptor conformation [54]. Since most X-ray structures of GPCRs reported to
16
17 date represent the inactive, antagonist-bound conformation, it cannot be excluded that
18
19 one or more cysteine residues might be involved in allosteric disulfide bonds and would
20
21 either be reduced in the active receptor conformation or could have formed artificially
22
23 during the crystallization process. Usually allosteric disulfide bonds are controlled by
24
25 catalytic disulfides of oxidoreductases, which are regulated through changes in the
26
27 oxidizing environment, e.g. through oxidative stress [54]. The fact that the structurally
28
29 different ligands - PSB-603, NECA, and BAY60-6583 - resulted in different changes in
30
31 IC_{50} - or EC_{50} (decreased or increased values) in the C154S mutant as compared to the
32
33 wild-type receptor indicates that C154 may be directly or indirectly involved in ligand
34
35 binding. However, this hypothesis cannot be confirmed by our homology model.
36
37
38
39
40
41
42
43
44

45 Free cysteine residues can also be involved in metal ion complexation, e.g. with Zn^{2+} ,
46
47 Pb^{2+} or Hg^{2+} . So far, reports about the role of metal ion complexation in the regulation of
48
49 GPCRs are scarce. Inhibitory effects of Zn^{2+} on ligand binding at the serotonin receptor
50
51 $5-HT_{1A}$ have been reported; the physiological significance, however, remained unclear
52
53 [59]. A few other studies also showed allosteric effects of zinc ions on ligand binding at
54
55 GPCRs (dopamine, metabotropic glutamate and β 2-adrenergic receptors) with likewise
56
57
58
59
60
61
62
63
64
65

1
2
3
4 unresolved physiological significance [60-61]. For several receptors, involvement of
5
6 cysteine residues in dimerization has been shown. In these cases, however, cysteine
7
8 residues were exclusively localized in the transmembrane domains or in intracellular
9
10 loops [62-63].
11
12
13
14
15

16 In summary, we showed that the conserved disulfide bond between C3.25 in TMD3 and
17
18 C45.50 in ECL2 is essential for adenosine A_{2B} receptor ligand binding and function and
19
20 it also appears to improve transport of the receptors to the plasma membrane.
21
22

23 Furthermore we have strong evidence that all other cysteine residues in the ECL2 are
24
25 not involved in disulfide bond formation and if they were, that those bonds would not
26
27 have any effects, neither on ligand binding, nor on receptor function. Only Cys154
28
29 appears to have small, significant effects on ligand binding. Thus, the cysteine residues
30
31 in the ECL2 of the A_{2B} receptor may serve very different roles from those of the
32
33 extracellular cysteine residues in the A_{2A} receptor.
34
35
36
37
38
39

40 **Acknowledgements**

41
42
43
44

45 A.C.S., D.T., and C.E.M. are supported by the state of NRW (NRW International
46
47 Research Graduate School BIOTECH-PHARMA). T.B. was supported by a stipend
48
49 provided by the Bischöfliche Studienförderung Cusanuswerk. We would like to thank
50
51 Susan Jean Johns for upgrading the TOPO2 program to fulfill our needs for more colors
52
53 in the topology model. We are also grateful to Dr. Thomas Krahn, Bayer Healthcare
54
55 (Germany) for providing BAY60-6583.
56
57
58
59
60
61
62
63
64
65

References

- [1] Burnstock G. Purine and pyrimidine receptors. *Cell Mol Life Sci* 2007;64:1471-83.
- [2] Brunschweiler A, Müller CE. P2 receptors activated by uracil nucleotides--an update. *Curr Med Chem* 2006;13:289-312.
- [3] Fredholm BB, Ijzerman AP, Jacobson KA, Linden J, Müller CE. Nomenclature and Classification of Adenosine Receptors - An update. *Pharmacol Rev* 2011;63:1-34.
- [4] Schulte G, Fredholm BB. Signalling from adenosine receptors to mitogen-activated protein kinases. *Cell Signal* 2003;15:813-27.
- [5] Linden J, Thai T, Figler H, Jin X, Robeva AS. Characterization of human A_{2B} adenosine receptors: radioligand binding, western blotting, and coupling to G(q) in human embryonic kidney 293 cells and HMC-1 mast cells. *Mol Pharmacol* 1999;56:705-13.
- [6] Feoktistov I, Biaggioni I. Adenosine A_{2B} receptors. *Pharmacol Rev* 1997;49:381-402.
- [7] Mirabet M, Mallol J, Lluís C, Franco R. Calcium mobilization in Jurkat cells via A_{2b} adenosine receptors. *Br J Pharmacol* 1997;122:1075-82.
- [8] Pearson G, Robinson F, Beers Gibson T, Xu BE, Karandikar M, Berman K, et al. Mitogen-activated protein (MAP) kinase pathways: regulation and physiological functions. *Endocr Rev* 2001;22:153-83.
- [9] Donoso MV, Lopez R, Miranda R, Briones R, Huidobro-Toro JP. A_{2B} adenosine receptor mediates human chorionic vasoconstriction and signals through arachidonic acid cascade. *Am J Physiol Heart Circ Physiol* 2005;288:H2439-49.
- [10] Müller CE, Jacobson KA. Recent developments in adenosine receptor ligands and their potential as novel drugs. *Biochim Biophys Acta* 2010; 1808:1290-308.
- [11] Borrmann T, Hinz S, Bertarelli DC, Li W, Florin NC, Scheiff AB, et al. 1-alkyl-8-(piperazine-1-sulfonyl)phenylxanthines: development and characterization of adenosine A_{2B} receptor antagonists and a new radioligand with subnanomolar affinity and subtype specificity. *J Med Chem* 2009;52:3994-4006.
- [12] Yan L, Burbiel JC, Maass A, Müller CE. Adenosine receptor agonists: from basic medicinal chemistry to clinical development. *Expert Opin Emerg Drugs* 2003;8:537-76.
- [13] Baraldi PG, Tabrizi MA, Fruttarolo F, Romagnoli R, Preti D. Recent improvements in the development of A(2B) adenosine receptor agonists. *Purinergic Signal* 2008;4:287-303. Epub 2008 Apr 29.
- [14] Fredholm BB. Adenosine, an endogenous distress signal, modulates tissue damage and repair. *Cell Death Differ* 2007;14:1315-23.
- [15] Kong T, Westerman KA, Faigle M, Eltzschig HK, Colgan SP. HIF-dependent induction of adenosine A_{2B} receptor in hypoxia. *FASEB J* 2006;20:2242-50.
- [16] Beukers MW, van Oppenraaij J, van der Hoorn PP, Blad CC, den Dulk H, Brouwer J, et al. Random mutagenesis of the human adenosine A_{2B} receptor followed by growth selection in yeast. Identification of constitutively active and gain of function mutations. *Mol Pharmacol* 2004;65:702-10.
- [17] Ryzhov S, Zaynagetdinov R, Goldstein AE, Novitskiy SV, Dikov MM, Blackburn MR, et al. Effect of A_{2B} adenosine receptor gene ablation on proinflammatory adenosine signaling in mast cells. *J Immunol* 2008;180:7212-20.

- 1
2
3
4 [18] Trincavelli ML, Marroni M, Tuscano D, Ceruti S, Mazzola A, Mitro N, et al.
5 Regulation of A2B adenosine receptor functioning by tumour necrosis factor α in
6 human astroglial cells. *J Neurochem* 2004;91:1180-90.
- 7 [19] Ryzhov S, Novitskiy SV, Zaynagetdinov R, Goldstein AE, Carbone DP, Biaggioni
8 I, et al. Host A(2B) adenosine receptors promote carcinoma growth. *Neoplasia*
9 2008;10:987-95.
- 10 [20] Volpini R, Costanzi S, Vittori S, Cristalli G, Klotz KN. Medicinal chemistry and
11 pharmacology of A2B adenosine receptors. *Curr Top Med Chem* 2003;3:427-43.
- 12 [21] Pastorin G, Federico S, Paoletta S, Corradino M, Cateni F, Cacciari B, et al.
13 Synthesis and pharmacological characterization of a new series of 5,7-
14 disubstituted-[1,2,4]triazolo[1,5-a][1,3,5]triazine derivatives as adenosine receptor
15 antagonists: A preliminary inspection of ligand-receptor recognition process.
16 *Bioorg Med Chem* 2010;18:2524-36.
- 17 [22] Pastorin G, Da Ros T, Spalluto G, Deflorian F, Moro S, Cacciari B, et al.
18 Pyrazolo[4,3-e]-1,2,4-triazolo[1,5-c]pyrimidine derivatives as adenosine receptor
19 antagonists. Influence of the N5 substituent on the affinity at the human A₃ and
20 A_{2B} adenosine receptor subtypes: a molecular modeling investigation. *Journal of*
21 *Medicinal Chemistry* 2003;46:4287-96.
- 22 [23] Beukers MW, den Dulk H, van Tilburg EW, Brouwer J, Ijzerman AP. Why are
23 A(2B) receptors low-affinity adenosine receptors? Mutation of Asn273 to Tyr
24 increases affinity of human A(2B) receptor for 2-(1-Hexynyl)adenosine. *Mol*
25 *Pharmacol* 2000;58:1349-56.
- 26 [24] Matharu AL, Mundell SJ, Benovic JL, Kelly E. Rapid agonist-induced
27 desensitization and internalization of the A(2B) adenosine receptor is mediated
28 by a serine residue close to the COOH terminus. *J Biol Chem* 2001;276:30199-
29 207.
- 30 [25] Peeters MC, van Westen GJ, Guo D, Wisse LE, Müller CE, Beukers MW, et al.
31 GPCR structure and activation: an essential role for the first extracellular loop in
32 activating the adenosine A_{2B} receptor. *FASEB J* 2010;4:4.
- 33 [26] Ivanov AA, Palyulin VA, Zefirov NS. Computer aided comparative analysis of the
34 binding modes of the adenosine receptor agonists for all known subtypes of
35 adenosine receptors. *J Mol Graph Model* 2007;25:740-54.
- 36 [27] Ivanov AA, Baskin, II, Palyulin VA, Piccagli L, Baraldi PG, Zefirov NS. Molecular
37 modeling and molecular dynamics simulation of the human A_{2B} adenosine
38 receptor. The study of the possible binding modes of the A_{2B} receptor
39 antagonists. *J Med Chem* 2005;48:6813-20.
- 40 [28] Kim YC, de Zwart M, Chang L, Moro S, von Frijtag Drabbe Kunzel JK, Melman N,
41 et al. Derivatives of the triazoloquinazoline adenosine antagonist (CGS 15943)
42 having high potency at the human A_{2B} and A₃ receptor subtypes. *Journal of*
43 *Medicinal Chemistry* 1998;41:2835-45.
- 44 [29] Sherbiny FF, Schiedel AC, Maass A, Müller CE. Homology modelling of the
45 human adenosine A2B receptor based on X-ray structures of bovine rhodopsin,
46 the beta2-adrenergic receptor and the human adenosine A_{2A} receptor. *J Comput*
47 *Aided Mol Des* 2009;23:807-28.
- 48 [30] Ballesteros J, Weinstein, H. Integrated methods for the construction of three-
49 dimensional models of structure-function relations in G protein-coupled receptors.
50 *Meth Neurosci* 1995;25:366-428.
- 51
52
53
54
55
56
57
58
59
60
61
62
63
64
65

- 1
2
3
4 [31] de Graaf C, Foata N, Engkvist O, Rognan D. Molecular modeling of the second
5 extracellular loop of G-protein coupled receptors and its implication on structure-
6 based virtual screening. *Proteins* 2008;71:599-620.
7
8 [32] Avlani VA, Gregory KJ, Morton CJ, Parker MW, Sexton PM, Christopoulos A.
9 Critical Role for the Second Extracellular Loop in the Binding of Both Orthosteric
10 and Allosteric G Protein-coupled Receptor Ligands. *J Biol Chem*
11 2007;282:25677-86.
12
13 [33] <http://www.ebi.ac.uk/Tools/clustalw2/>. (27.01.2011).
14 [34] <http://www.ebi.ac.uk/Tools/emboss/align/>. (27.01.2011).
15 [35] <http://www.cbs.dtu.dk/services/NetNGlyc/>. (27.01.2011).
16 [36] <http://www.sacs.ucsf.edu/TOPO2/>. (27.01.2011).
17 [37] <http://modbase.compbio.ucsf.edu/modloop/>. (27.01.2011).
18 [38] <http://ambermd.org/>. (27.01.2011).
19 [39] <http://www.ebi.ac.uk/thornton-srv/software/PROCHECK/>. (27.01.2011).
20 [40] Sippl MJ. Recognition of errors in three-dimensional structures of proteins.
21 *Proteins* 1993;17:355-62.
22
23 [41] Lowry OH, Rosebrough NJ, Farr AL, Randall RJ. Protein measurement with the
24 Folin phenol reagent. *J Biol Chem* 1951;193:265-75.
25
26 [42] Hillmann P, Ko GY, Spinrath A, Raulf A, von Kugelgen I, Wolff SC, et al. Key
27 determinants of nucleotide-activated G protein-coupled P2Y(2) receptor function
28 revealed by chemical and pharmacological experiments, mutagenesis and
29 homology modeling. *J Med Chem* 2009;52:2762-75.
30
31 [43] Motulsky HJ, Christopoulos A. Fitting models to biological data using linear and
32 nonlinear regression. San Diego: GraphPad Software Inc., 2003.
33
34 [44] Nordstedt C, Fredholm BB. A modification of a protein-binding method for rapid
35 quantification of cAMP in cell-culture supernatants and body fluid. *Analytical*
36 *Biochemistry* 1990;189:231-4.
37
38 [45] Jaakola VP, Griffith MT, Hanson MA, Cherezov V, Chien EY, Lane JR, et al. The
39 2.6 angstrom crystal structure of a human A_{2A} adenosine receptor bound to an
40 antagonist. *Science* 2008;322:1211-7.
41
42 [46] Peeters MC, van Westen GJ, Li Q, Ijzerman AP. Importance of the extracellular
43 loops in G protein-coupled receptors for ligand recognition and receptor
44 activation. *Trends Pharmacol Sci* 2011;32:35-42.
45
46 [47] Karnik SS, Sakmar TP, Chen HB, Khorana HG. Cysteine residues 110 and 187
47 are essential for the formation of correct structure in bovine rhodopsin.
48 *Proceedings of the National Academy of Sciences of the United States of*
49 *America* 1988;85:8459-63.
50
51 [48] Ding Z, Kim S, Dorsam RT, Jin J, Kunapuli SP. Inactivation of the human P2Y₁₂
52 receptor by thiol reagents requires interaction with both extracellular cysteine
53 residues, Cys17 and Cys270. *Blood* 2003;101:3908-14.
54
55 [49] Shi L, Javitch JA. The second extracellular loop of the dopamine D2 receptor
56 lines the binding-site crevice. *Proc Natl Acad Sci U S A* 2004;101:440-5.
57
58 [50] Duong HT, Gao ZG, Jacobson KA. Nucleoside modification and concerted
59 mutagenesis of the human A₃ adenosine receptor to probe interactions between
60 the 2-position of adenosine analogs and Gln167 in the second extracellular loop.
61 *Nucleosides Nucleotides Nucleic Acids* 2005;24:1507-17.
62
63
64
65

- 1
2
3
4 [51] Bokoch MP, Zou Y, Rasmussen SG, Liu CW, Nygaard R, Rosenbaum DM, et al.
5 Ligand-specific regulation of the extracellular surface of a G-protein-coupled
6 receptor. *Nature* 2010;463:108-12.
7
8 [52] Ai LS, Liao F. Mutating the four extracellular cysteines in the chemokine receptor
9 CCR6 reveals their differing roles in receptor trafficking, ligand binding, and
10 signaling. *Biochemistry* 2002;41:8332-41.
11
12 [53] McGinnes LW, Morrison TG. Disulfide bond formation is a determinant of
13 glycosylation site usage in the hemagglutinin-neuraminidase glycoprotein of
14 Newcastle disease virus. *J Virol* 1997;71:3083-9.
15
16 [54] Azimi I, Wong JW, Hogg PJ. Control of mature protein function by allosteric
17 disulfide bonds. *Antioxid Redox Signal* 2011;14:113-26.
18
19 [55] Rubenstein LA, Zauhar RJ, Lanzara RG. Molecular dynamics of a biophysical
20 model for beta2-adrenergic and G protein-coupled receptor activation. *J Mol
21 Graph Model* 2006;25:396-409.
22
23 [56] Mercier RW, Pei Y, Pandarinathan L, Janero DR, Zhang J, Makriyannis A. hCB2
24 ligand-interaction landscape: cysteine residues critical to biarylpyrazole
25 antagonist binding motif and receptor modulation. *Chem Biol* 2010;17:1132-42.
26
27 [57] Varani K, Caramori G, Vincenzi F, Tosi A, Barczyk A, Contoli M, et al.
28 Oxidative/nitrosative stress selectively altered A2B adenosine receptors in
29 chronic obstructive pulmonary disease. *FASEB J* 2009;14:14.
30
31 [58] Goddard WA, 3rd, Kim SK, Li Y, Trzaskowski B, Griffith AR, Abrol R. Predicted
32 3D structures for adenosine receptors bound to ligands: comparison to the crystal
33 structure. *J Struct Biol* 2010;170:10-20.
34
35 [59] Barrondo S, Salles J. Allosteric modulation of 5-HT(1A) receptors by zinc: Binding
36 studies. *Neuropharmacology* 2009;56:455-62. Epub 2008 Oct 14.
37
38 [60] Schetz JA, Chu A, Sibley DR. Zinc modulates antagonist interactions with D2-like
39 dopamine receptors through distinct molecular mechanisms. *J Pharmacol Exp
40 Ther* 1999;289:956-64.
41
42 [61] Elling CE, Frimurer TM, Gerlach LO, Jorgensen R, Holst B, Schwartz TW. Metal
43 ion site engineering indicates a global toggle switch model for seven-
44 transmembrane receptor activation. *J Biol Chem* 2006;281:17337-46. Epub 2006
45 Mar 27.
46
47 [62] Klco JM, Lassere TB, Baranski TJ. C5a receptor oligomerization. I. Disulfide
48 trapping reveals oligomers and potential contact surfaces in a G protein-coupled
49 receptor. *J Biol Chem* 2003;278:35345-53.
50
51 [63] Berthouze M, Rivail L, Lucas A, Ayoub MA, Russo O, Sicsic S, et al. Two
52 transmembrane Cys residues are involved in 5-HT4 receptor dimerization.
53 *Biochem Biophys Res Commun* 2007;356:642-7.
54
55
56
57
58
59
60
61
62
63
64
65

Table 1. Evaluation of the goodness of different A_{2A} and A_{2B} receptor models after simulation

	m1 A _{2A}	m2 A _{2A}	m1 A _{2B}	m2 A _{2B}	m3 A _{2B}	m4 A _{2B}
disulfide bonds fixed before simulation	C77-C166	C71-C159 C74-C146 C77-C166 C259-C262	C78-C171	C72-C167 C78-C171	C72-C166 C78-C171	C72-C167 C78-C171 C154-C166
PROCHECK psi/phi angels ^a	1.1	0.4	0.7	0.7	0.7	1.0
PROSAII Z-score ^b	-4.3	-4.11	-4.06	-3.91	-4.17	-4.42
RMSD ^c relative to the A _{2A} crystal structure [Å]	1.0	0.8	1.3	1.9	1.7	1.7
RMSD relative to initial structure [Å]	0.9	0.8	0.7	1.0	0.8	0.8

^apsi (angle between carbon and carbonyl) and phi angels (angle between carbon and nitrogen) are determined using a Ramachandran plot, which is a way to visualize the dihedral angles (psi against phi) of amino acid residues in protein structures. Lower values indicate better quality.

^bThe Z-score indicates the overall model quality, its value is displayed in a plot which shows the local model quality by plotting energies as a function of the amino acid sequence position. In general, positive values correspond to problematic parts of the input structure, negative values indicate good quality.

^cRMSD: root mean square distance. Lower overall values indicate good accordance between two models.

Table 2: Affinities of the antagonist PSB-603 and the agonist NECA at the human A_{2B} receptor mutants and the wt receptor determined in radioligand binding studies versus [³H]PSB-603 (0.3 nM). Data are means ± SEM of three independent experiments unless otherwise noted.

wt or mutant	PSB-603 IC ₅₀ ± SEM (nM)	NECA IC ₅₀ ± SEM (nM)
wt	2.39 ± 0.71 ^a	5300 ± 946 ^b
C78S	- ^c	- ^c
C154S	19.0 ± 4.3 ^{***}	4970 ± 490 ^{ns}
C166S	1.41 ± 0.15 ^{ns}	4253 ± 766 ^{ns}
C167S	1.60 ± 0.38 ^{ns}	2933 ± 121 ^{ns}
C166S-C167S	5.49 ± 1.30 ^{d ns}	3920 ± 517 ^{ns}
C171S	- ^c	- ^c

^a n=6; ^b n=5; ^c could not be determined since [³H]PSB-603 did not show high affinity binding to the mutants; ^d n=2; Results of two-tailed t-test: ^{ns} not significantly different from wildtype, ^{***} p < 0.001

Table 3: EC₅₀ values determined for the agonists NECA and BAY60-6583 in cAMP accumulation assays at the wt and the mutants of the human A_{2B} receptor. Data are means ± SEM of three independent experiments unless otherwise noted.

wt or mutant	NECA		BAY60-6583	
	EC ₅₀ ± SEM (nM)	fold shift ^a	EC ₅₀ ± SEM (nM)	fold shift ^a
wt	58.1 ± 11.7 ^b		62.8 ± 7.3 ^c	
C78S	397 000 ± 7700 ***	6830	> 100 000 ***	> 1590
C154S	159 ± 29 **	2.7	35.9 *	0.6
C166S	71.1 ± 12.6 ^{ns}	1.2	26.8 ± 6.1 *	0.4
C167S	64.5 ± 6.5 ^{ns}	1.1	26.3 ± 5.5 *	0.4
C166S-C167S	94.1 ± 13.0 ^{ns}	1.6	40.6 ^{ns}	0.6
C171S	256 000 ± 28 900 ***	4400	> 100 000 ***	> 1590

^a The shift represents the ratio EC₅₀ (mutant) : EC₅₀ (wt); ^b n=6; ^c n=5; Results of a two-tailed t-test: ^{ns} not significantly different from wildtype, * p < 0.05, ** p < 0.01, *** p < 0.001

1
2
3
4 **Figure 1:** Topology model of the human A_{2B} receptor. The topology of the human A_{2B}
5
6 receptor is shown as a snakeplot diagram drawn with TOPO2 [36]. The amino acids are
7
8 shown in the one-letter code. Cysteine residues which were exchanged for serine by
9
10 site-directed mutagenesis are shown as squares and color-coded as follows: C78, red;
11
12 C154, purple, C166, cyan; C167, blue; C171, green. The two potential glycosylation
13
14 sites are shown as up-arrows: brown: N153; orange: N163. C72 (magenta) is shown as
15
16
17
18
19 hexagon.

20
21
22
23 **Figure 2: (A)** Alignments of the first and second extracellular loops of the human A_{2A}
24
25 and A_{2B} receptors. The alignment was done using Clustal W2 [33]. The following amino
26
27 acid residues are highlighted: magenta: C71^{A2A}/C72^{A2B}; red: conserved cysteine C3.25
28
29 in TMD3, C77^{A2A}/C78^{A2B}; purple: C146^{A2A}/C154^{A2B}; cyan: C166^{A2B}; blue:
30
31 C159^{A2A}/C167^{A2B}; green: C166^{A2A}/C171^{A2B}; potential N glycosylation sites: brown:
32
33 N153^{A2B}; orange: N161^{A2A}/N163^{A2B}; underlined: N glycosylation seqouns; bold and italic:
34
35 β-sheets; ECL: extracellular loop; * identical amino acid residue, : conserved amino acid
36
37 substitution; . semi-conserved amino acid substitution. Amino acid positions of cysteine
38
39 residues are given for the human A_{2A} and the A_{2B} receptor. **(B)** Cysteine residues
40
41 involved in disulfide bonds found in the crystal structure of the human A_{2A} receptor [45]
42
43 and cysteine residues involved in predicted disulfide bonds in the human A_{2B} receptor.
44
45
46
47
48
49
50
51
52

53 **Figure 3:** Molecular models of the human adenosine A_{2B} receptor. **(A)** Initial model
54
55 without fixed disulfide bonds (starting conformation). **(B)** Model 1 A_{2B} after simulation
56
57 with one fixed disulfide bond: C78-C171 (m1 A_{2B}). The following amino acids are shown
58
59
60
61
62
63
64
65

1
2
3
4 as stick models: magenta: C72; red: C78; purple: C154; cyan: C166; blue: C167; green:
5
6 C171; potential N glycosylation sites: brown: N153 and orange: N163.
7
8
9

10
11 **Figure 4:** Comparison of B-factors for the disulfide bond predictions of the four
12 simulated models of the human A_{2B} receptor and for model 2 of the human A_{2A} receptor.
13
14 B-factors indicate the true static or dynamic mobility of an atom, it can also indicate
15
16 where there are errors in model building. Higher values indicate higher mobility of
17
18 residues.
19
20
21
22
23
24
25

26 **Figure 5:** Effect of preincubation with DTT on A_{2B} receptor activity. NECA-induced
27 cAMP accumulation in CHO cells stably expressing the human A_{2B} receptor without and
28
29 with DTT pretreatment (10 mM DTT, 2 h at 37°C). Data points represent mean values
30
31 ± SEM from three independent experiments performed in triplicates. Determined EC₅₀
32
33 values: control: 36.6 ± 4.8 nM, DTT-pretreated: 2720 ± 570 nM.
34
35
36
37
38
39
40

41 **Figure 6:** Competition binding experiments of standard ligands at HA-tagged and
42 untagged human adenosine A_{2B} receptors. Radioligand binding experiments were
43
44 performed at membrane preparations of CHO cells stably expressing the human A_{2B}
45
46 receptor using the antagonist [³H]PSB-603 (0.3 nM) as a radioligand. Data points
47
48 represent means ± SEM of three independent experiments performed in triplicates. IC₅₀
49
50 and K_i values are listed in supplemental table 1. Results from untagged and HA-tagged
51
52 receptors were not significantly different.
53
54
55
56
57
58
59
60
61
62
63
64
65

1
2
3
4 **Figure 7:** Saturation binding of [³H]PSB-603 to human adenosine A_{2B} receptors (**A**)
5
6 without and (**B**) with HA tag, stably expressed in CHO cells. Data points represent
7
8 means ± SEM of three independent experiments performed in duplicates. K_D value for
9
10 untagged A_{2B} receptors: 0.403 ± 0.188 nM, for HA-tagged A_{2B} receptors: 0.473 ± 0.170
11
12 nM (not significantly different). Determined B_{max} values were 502 ± 57 fmol/mg protein
13
14 (**A**), and 283 ± 37 fmol/mg protein (**B**).
15
16
17
18
19
20

21 **Figure 8:** Agonist induced cAMP accumulation in CHO cells stably expressing HA-
22
23 tagged or untagged A_{2B} receptors using (**A**) NECA, or (**B**) BAY60-6583 as agonists.
24
25 Data points represent mean values ± SEM from three independent experiments
26
27 performed in duplicates. Corresponding EC₅₀ values are summarized in supplemental
28
29 table 1. Results from untagged and HA-tagged receptors were not significantly different.
30
31
32
33
34
35

36 **Figure 9:** Cell surface expression levels of mutant receptors in comparison to the wt A_{2B}
37
38 receptor determined by ELISA. Values were normalized versus values from cells
39
40 transfected with the empty plasmid, set at 0 % and values from cells expressing the wt
41
42 receptor, set at 100 %. Data represent the mean values ± SEM of two (C166S-C167S,
43
44 C171S), three (empty, C78S, C154S, C166S, C167S), or six (wt) independent
45
46 experiments performed in triplicates.
47
48
49
50
51
52

53 **Figure 10:** Agonist-induced cAMP accumulation studies in CHO cells stably expressing
54
55 the wt and cysteine mutants of the human A_{2B} receptor using (**A**) NECA, and (**B**)
56
57 BAY60-6583 as agonists. Data represent mean curves ± SEM from six (wt) or three
58
59
60
61
62
63
64
65

1
2
3
4 (mutants) independent experiments performed in duplicates. Corresponding EC₅₀ values
5
6 are summarized in table 3. The C78S and C171S mutants could not be activated by
7
8 BAY60-6583 at concentrations which were soluble (solubility < 30 μM).
9
10
11
12
13
14
15
16
17
18
19
20
21
22
23
24
25
26
27
28
29
30
31
32
33
34
35
36
37
38
39
40
41
42
43
44
45
46
47
48
49
50
51
52
53
54
55
56
57
58
59
60
61
62
63
64
65

Table 1. Evaluation of the goodness of different A_{2A} and A_{2B} receptor models after simulation

	m1 A_{2A}	m2 A_{2A}	m1 A_{2B}	m2 A_{2B}	m3 A_{2B}	m4 A_{2B}
disulfide bonds fixed before simulation	C77-C166	C71-C159 C74-C146 C77-C166 C259-C262	C78-C171	C72-C167 C78-C171	C72-C166 C78-C171	C72-C167 C78-C171 C154-C166
PROCHECK psi/phi angels ^a	1.1	0.4	0.7	0.7	0.7	1.0
PROSAII Z-score ^b	-4.3	-4.11	-4.06	-3.91	-4.17	-4.42
RMSD ^c relative to the A _{2A} crystal structure [Å]	1.0	0.8	1.3	1.9	1.7	1.7
RMSD relative to initial structure [Å]	0.9	0.8	0.7	1.0	0.8	0.8

^apsi (angle between carbon and carbonyl) and phi angels (angle between carbon and nitrogen) are determined using a Ramachandran plot, which is a way to visualize the dihedral angles (psi against phi) of amino acid residues in protein structures. Lower values indicate better quality.

^bThe Z-score indicates the overall model quality, its value is displayed in a plot which shows the local model quality by plotting energies as a function of the amino acid sequence position. In general, positive values correspond to problematic parts of the input structure, negative values indicate good quality.

^cRMSD: root mean square distance. Lower overall values indicate good accordance between two models.

Table 2: Affinities of the antagonist PSB-603 and the agonist NECA at the human A_{2B} receptor mutants and the wt receptor determined in radioligand binding studies versus [³H]PSB-603 (0.3 nM). Data are means ± SEM of three independent experiments unless otherwise noted.

wt or mutant	PSB-603	NECA
	IC ₅₀ ± SEM (nM)	IC ₅₀ ± SEM (nM)
wt	2.39 ± 0.71 ^a	5300 ± 946 ^b
C78S	- ^c	- ^c
C154S	19.0 ± 4.3 ^{***}	4970 ± 490 ^{ns}
C166S	1.41 ± 0.15 ^{ns}	4253 ± 766 ^{ns}
C167S	1.60 ± 0.38 ^{ns}	2933 ± 121 ^{ns}
C166S-C167S	5.49 ± 1.30 ^{d ns}	3920 ± 517 ^{ns}
C171S	- ^c	- ^c

^a n=6; ^b n=5; ^c could not be determined since [³H]PSB-603 did not show high affinity binding to the mutants; ^d n=2; Results of two-tailed t-test: ^{ns} not significantly different from wildtype, ^{***} p < 0.001

Table 3: EC₅₀ values determined for the agonists NECA and BAY60-6583 in cAMP accumulation assays at the wt and the mutants of the human A_{2B} receptor. Data are means ± SEM of three independent experiments unless otherwise noted.

wt or mutant	NECA		BAY60-6583	
	EC ₅₀ ± SEM (nM)	fold shift ^a	EC ₅₀ ± SEM (nM)	fold shift ^a
wt	58.1 ± 11.7 ^b		62.8 ± 7.3 ^c	
C78S	397 000 ± 7700 ***	6830	> 100 000 ***	> 1590
C154S	159 ± 29 **	2.7	35.9 *	0.6
C166S	71.1 ± 12.6 ^{ns}	1.2	26.8 ± 6.1 *	0.4
C167S	64.5 ± 6.5 ^{ns}	1.1	26.3 ± 5.5 *	0.4
C166S-C167S	94.1 ± 13.0 ^{ns}	1.6	40.6 ^{ns}	0.6
C171S	256 000 ± 28 900 ***	4400	> 100 000 ***	> 1590

^a The shift represents the ratio EC₅₀ (mutant) : EC₅₀ (wt); ^b n=6; ^c n=5; Results of a two-tailed t-test:

^{ns} not significantly different from wildtype, * p < 0.05, ** p < 0.01, *** p < 0.001

Figure 1

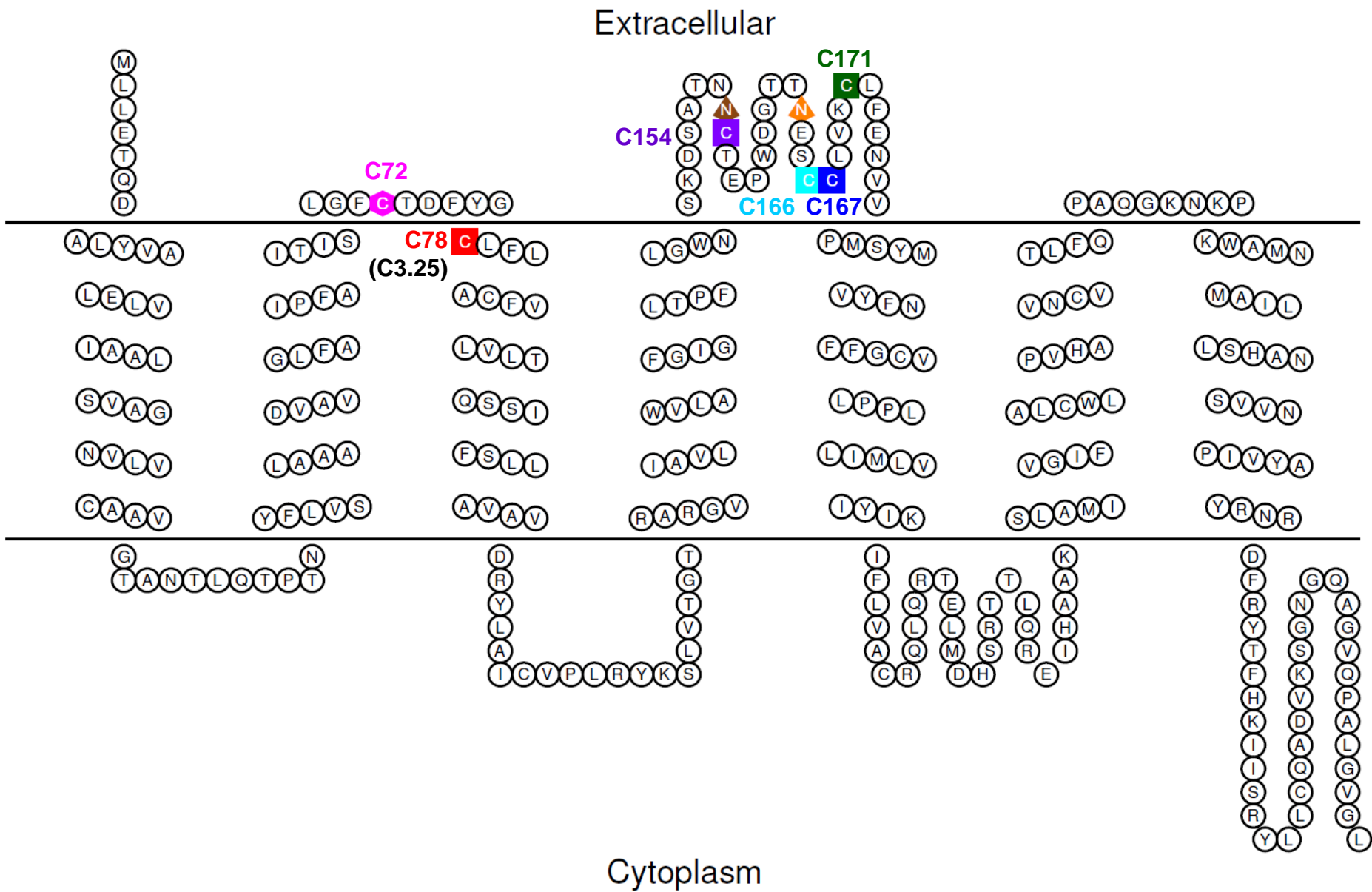
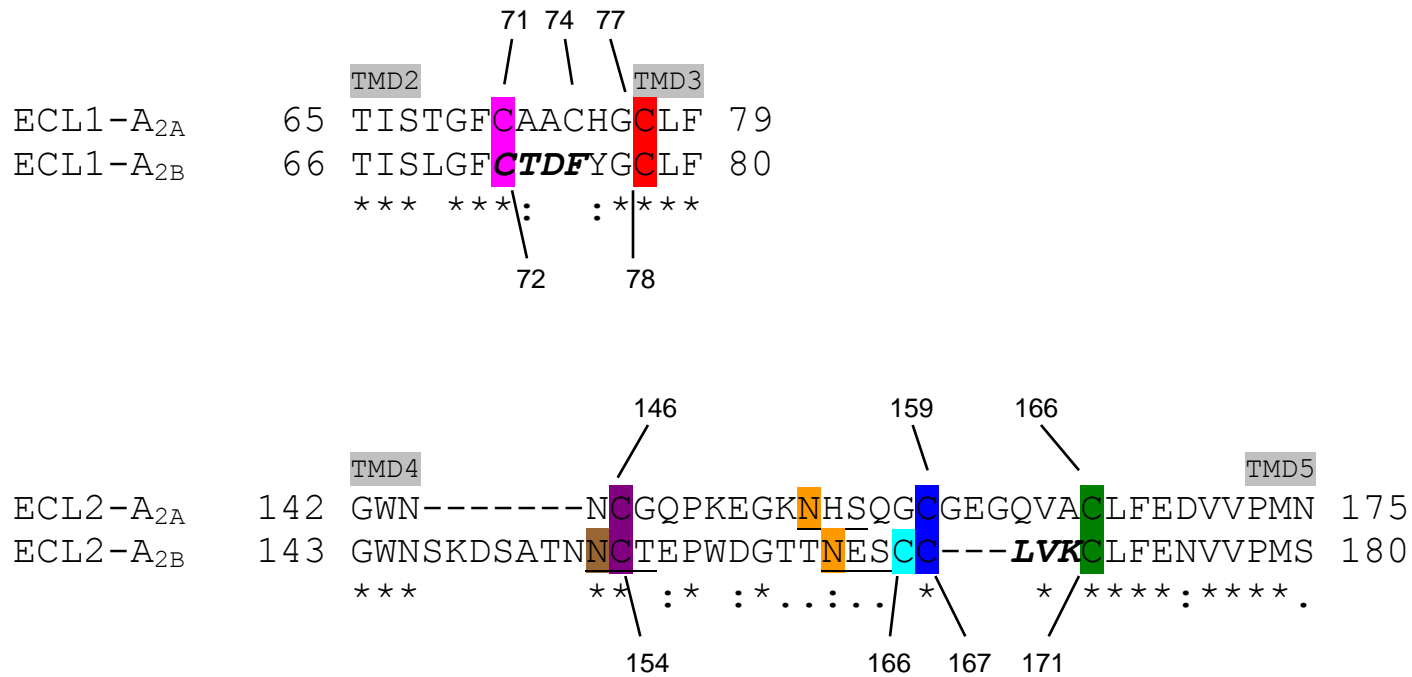


Figure 2

A



B

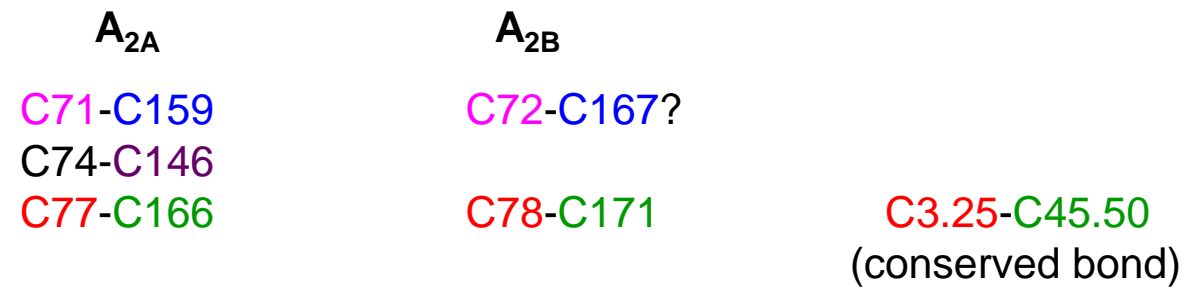
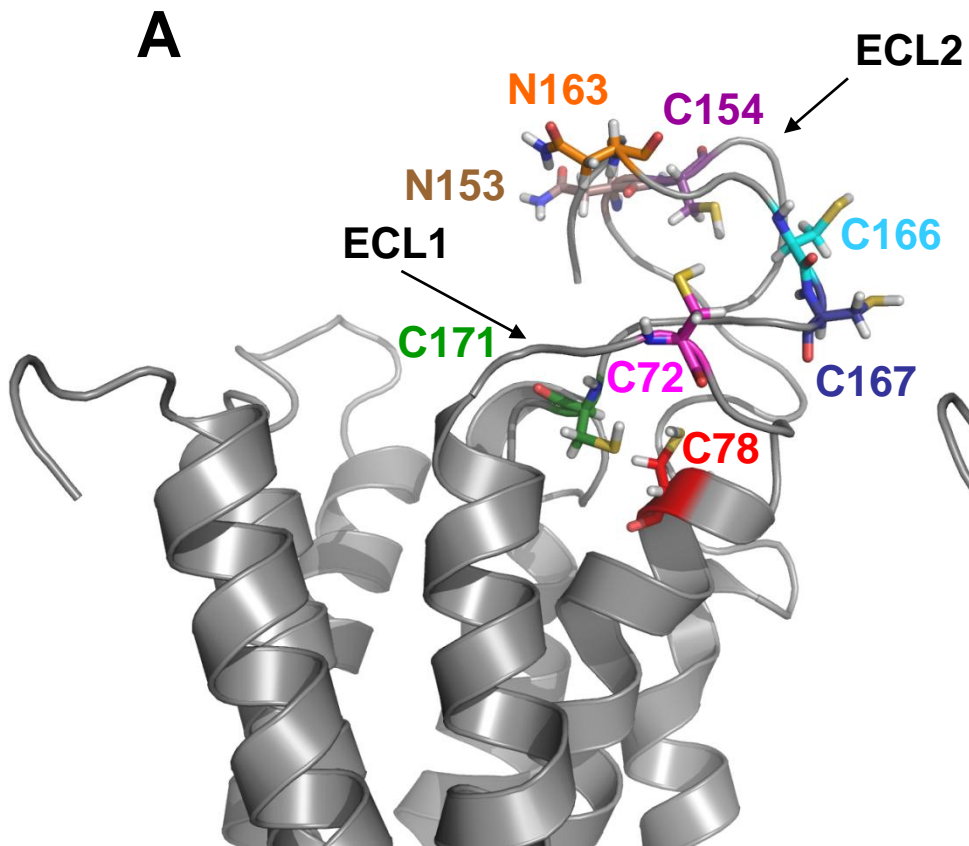


Figure 3

A



B

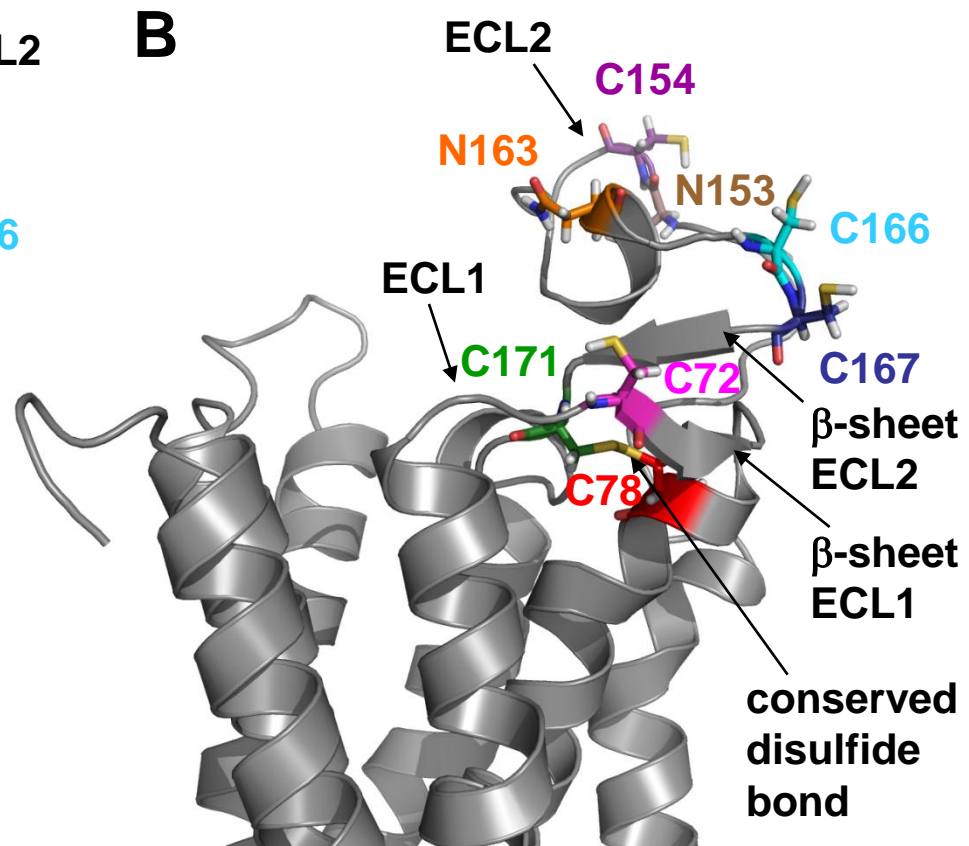


Figure 4
[Click here to download high resolution image](#)

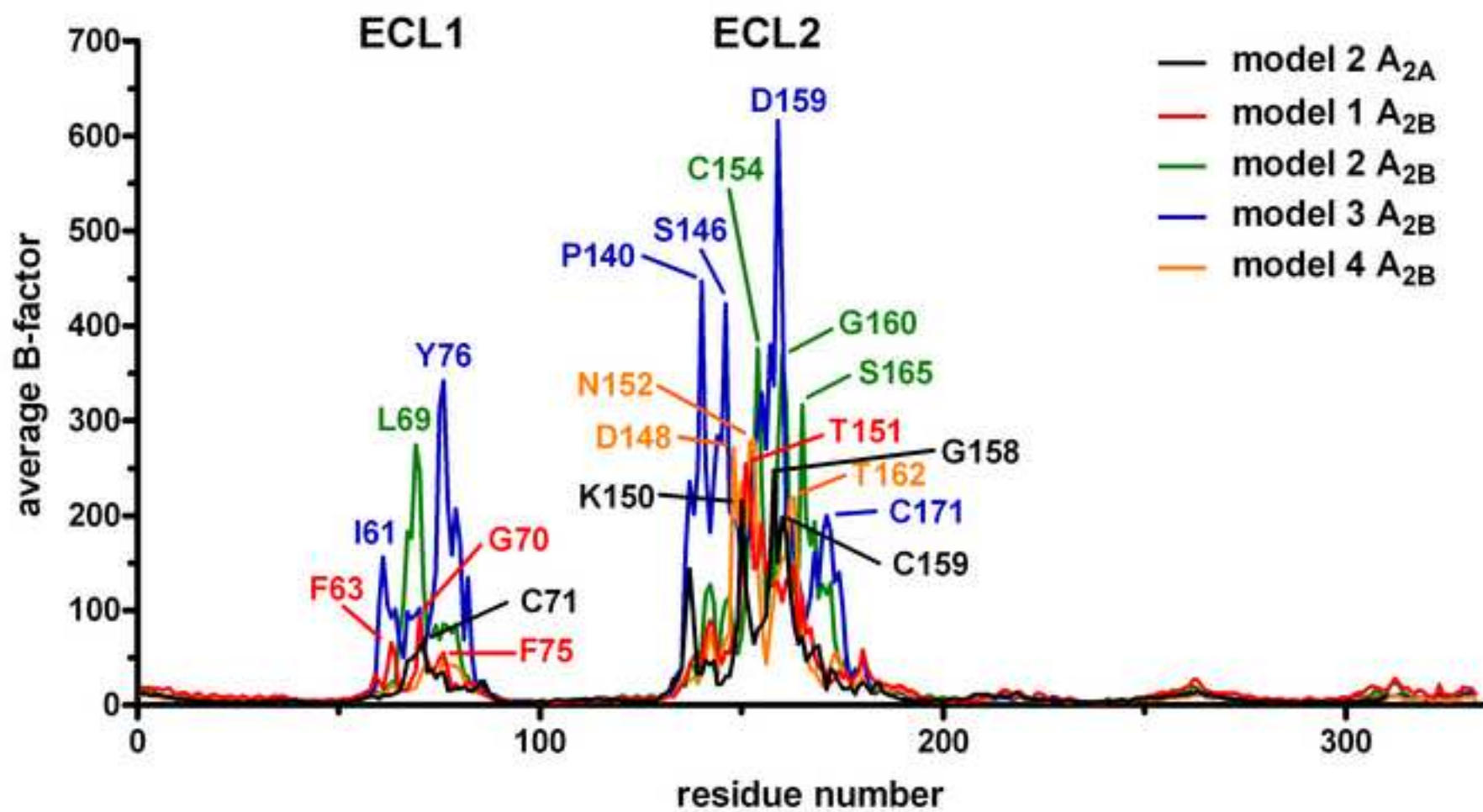


Figure 5
[Click here to download high resolution image](#)

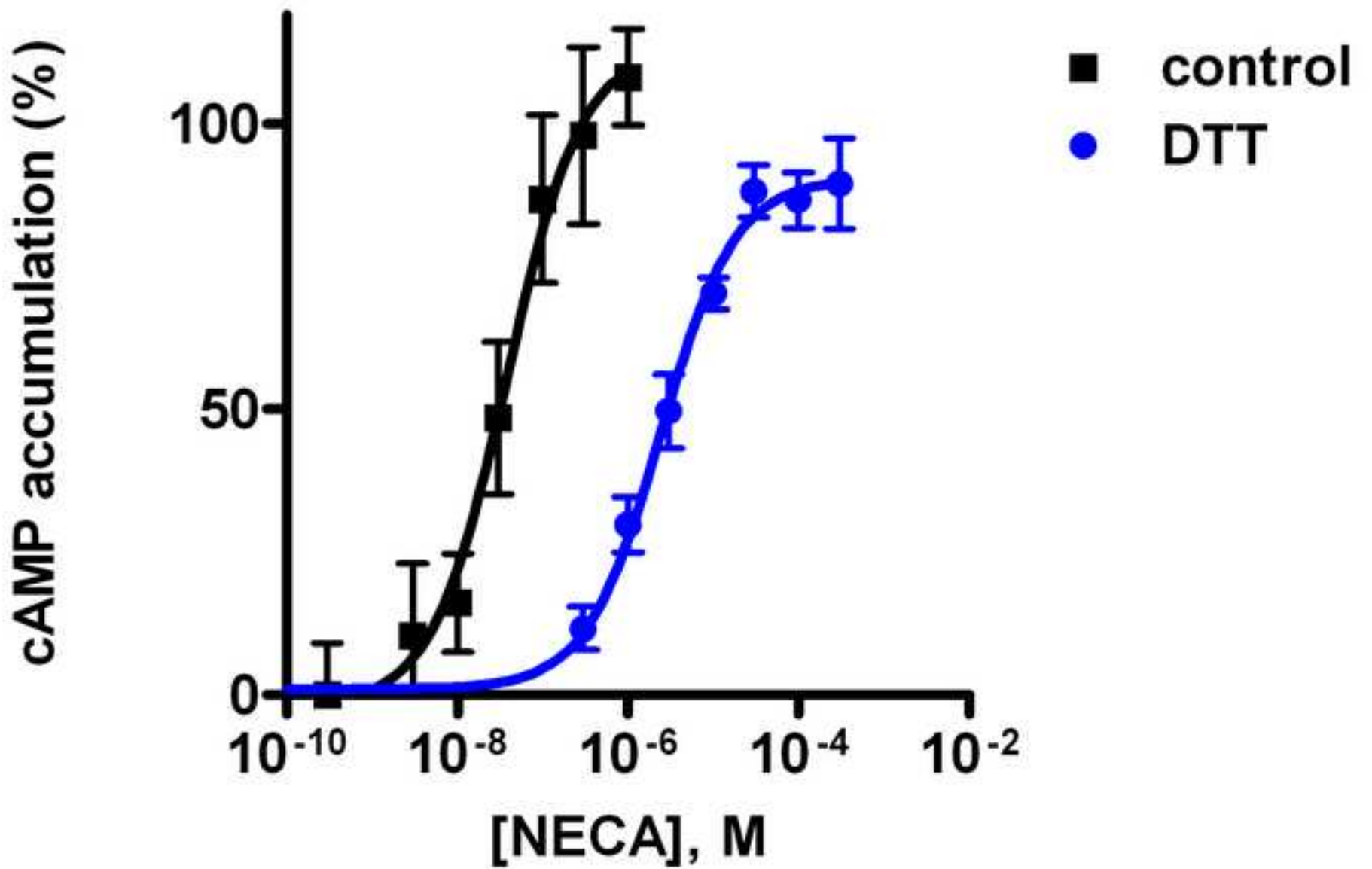
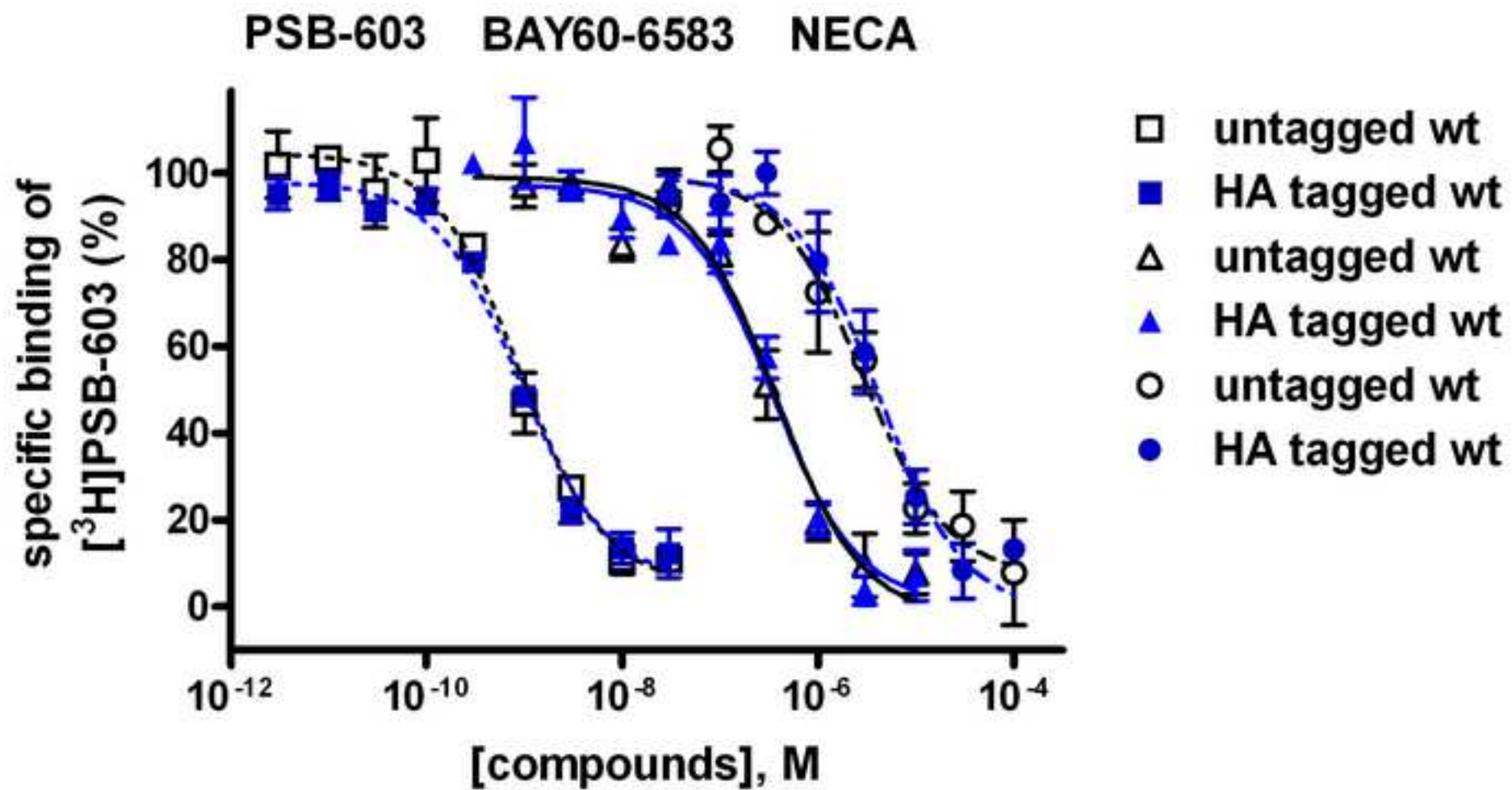
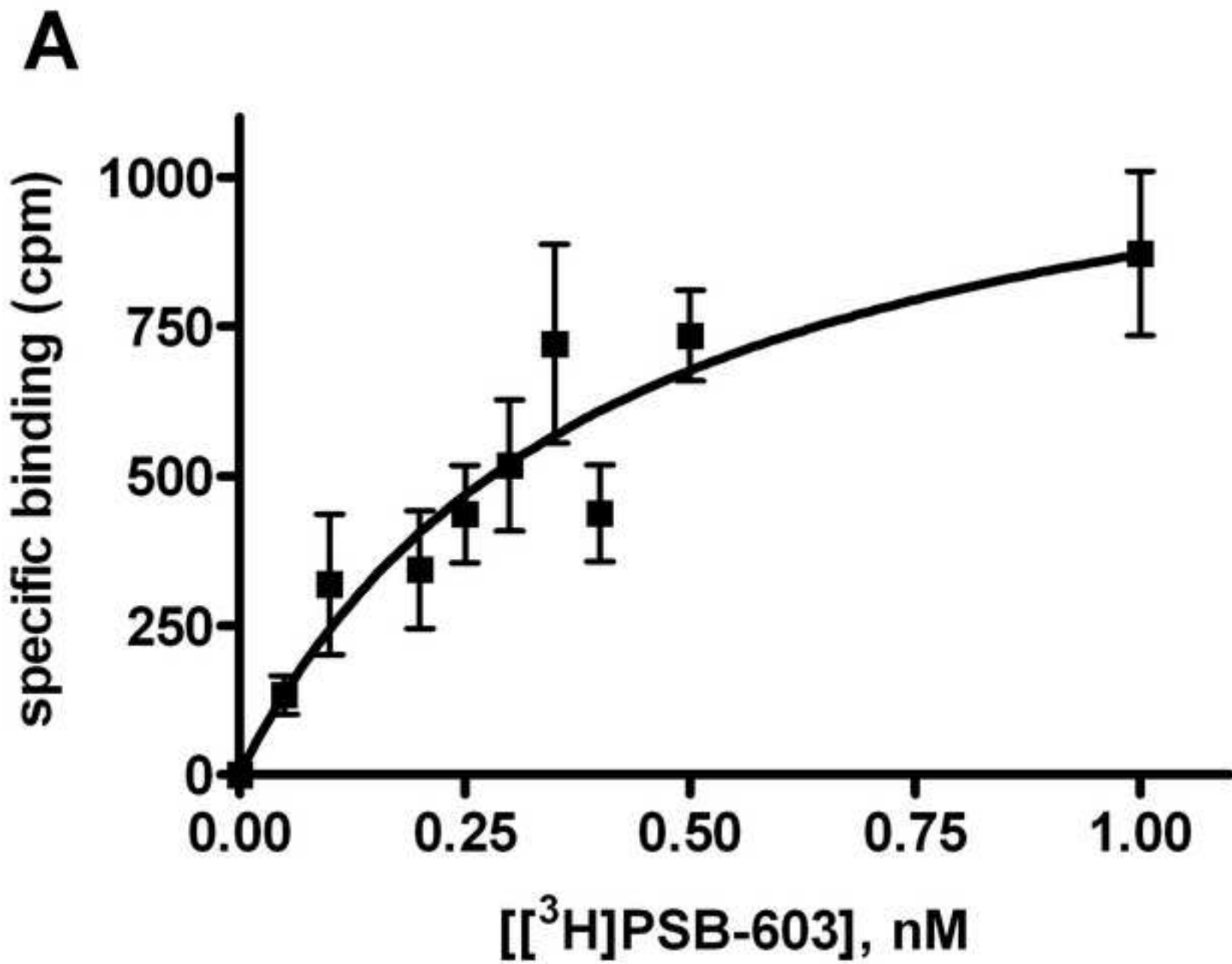


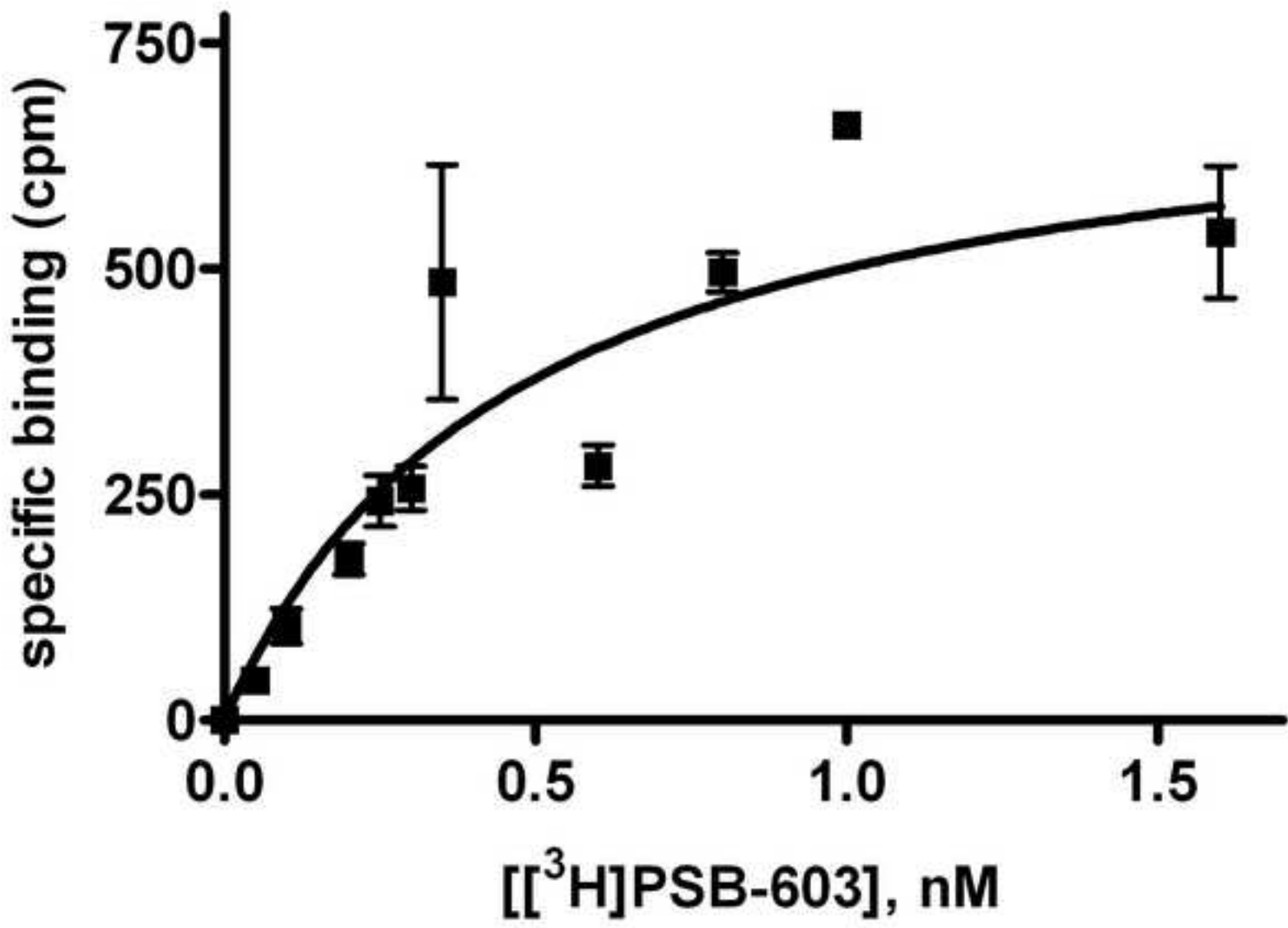
Figure 6
[Click here to download high resolution image](#)



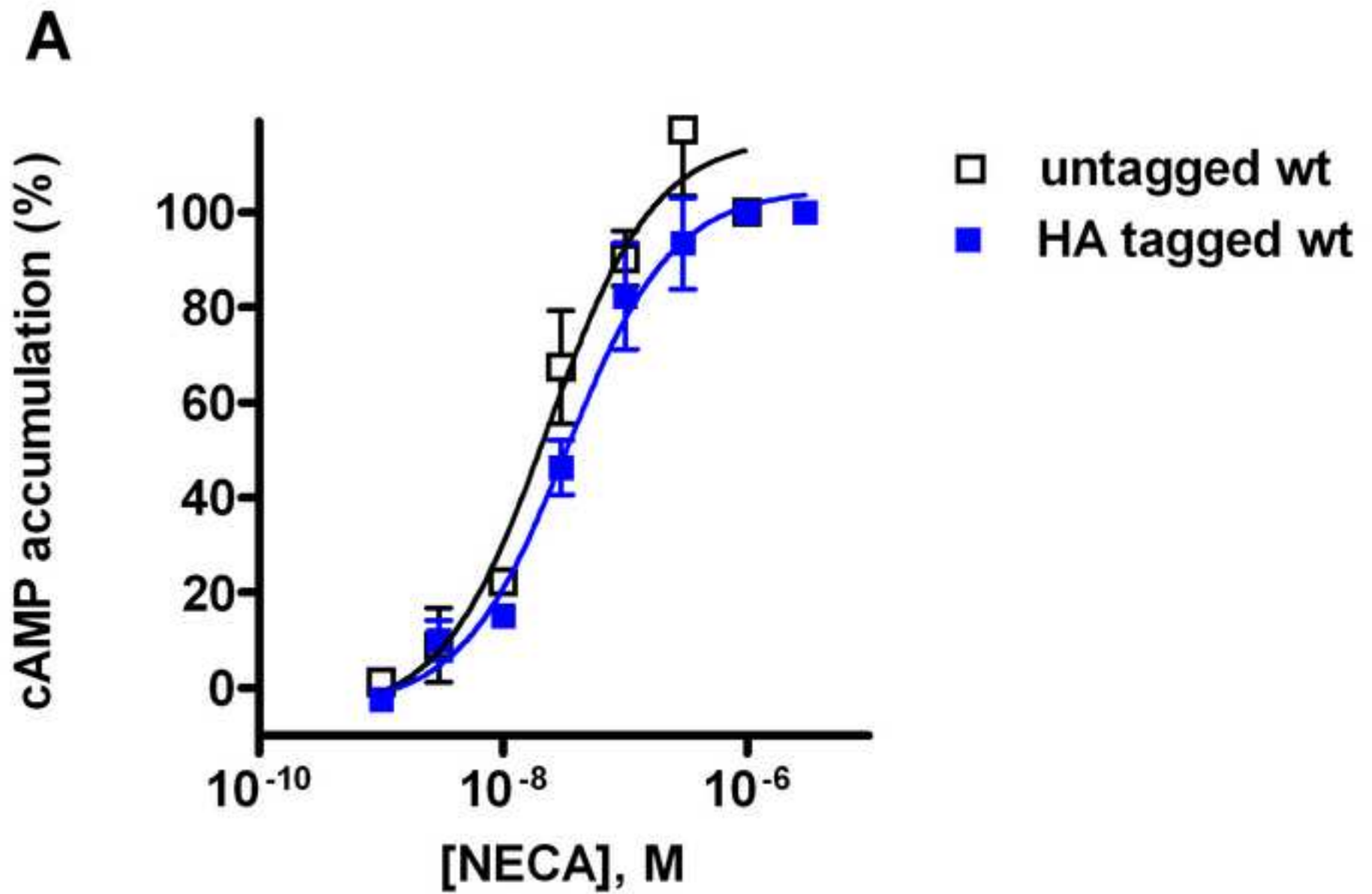
trip



B



crip



B

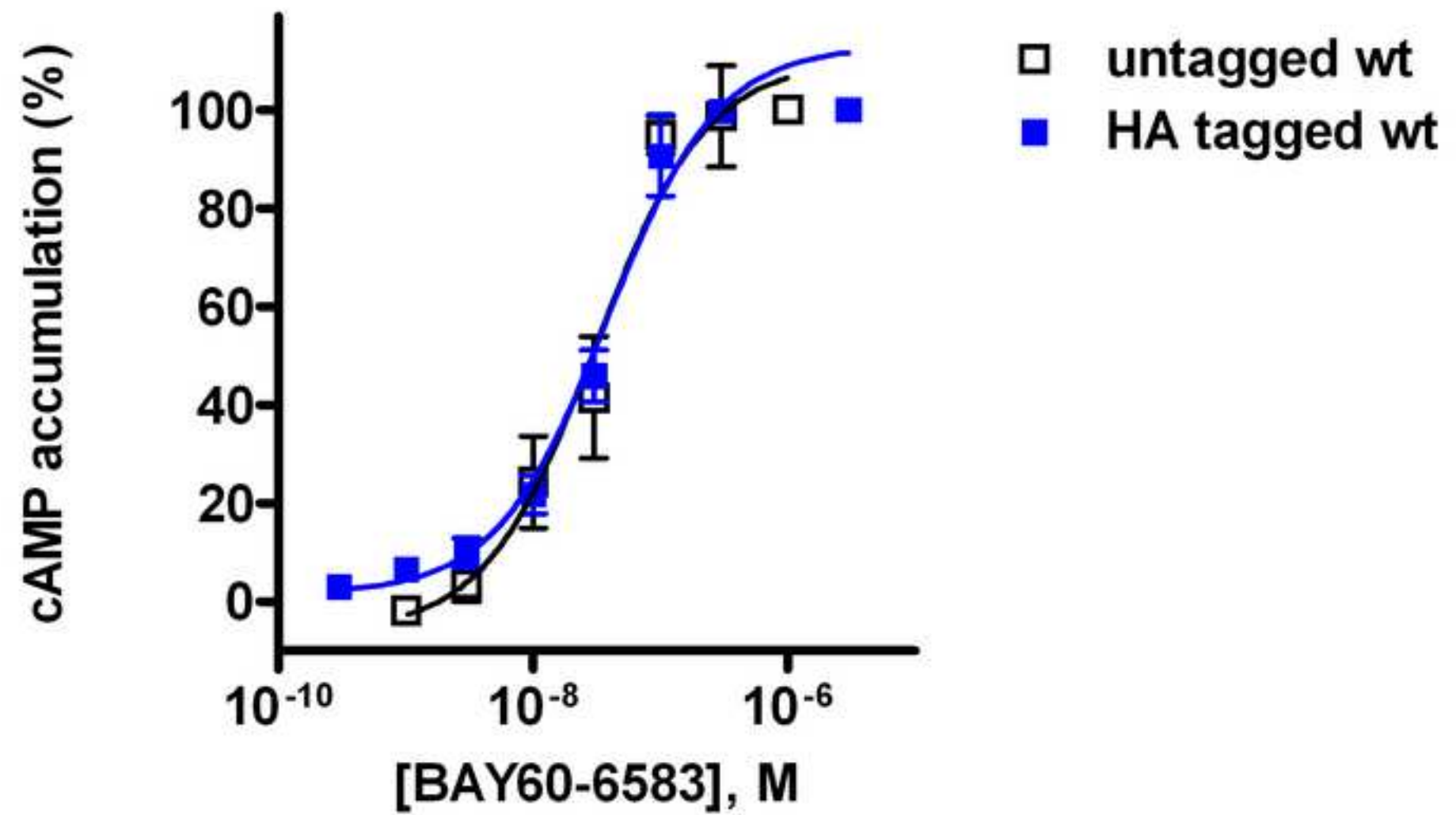
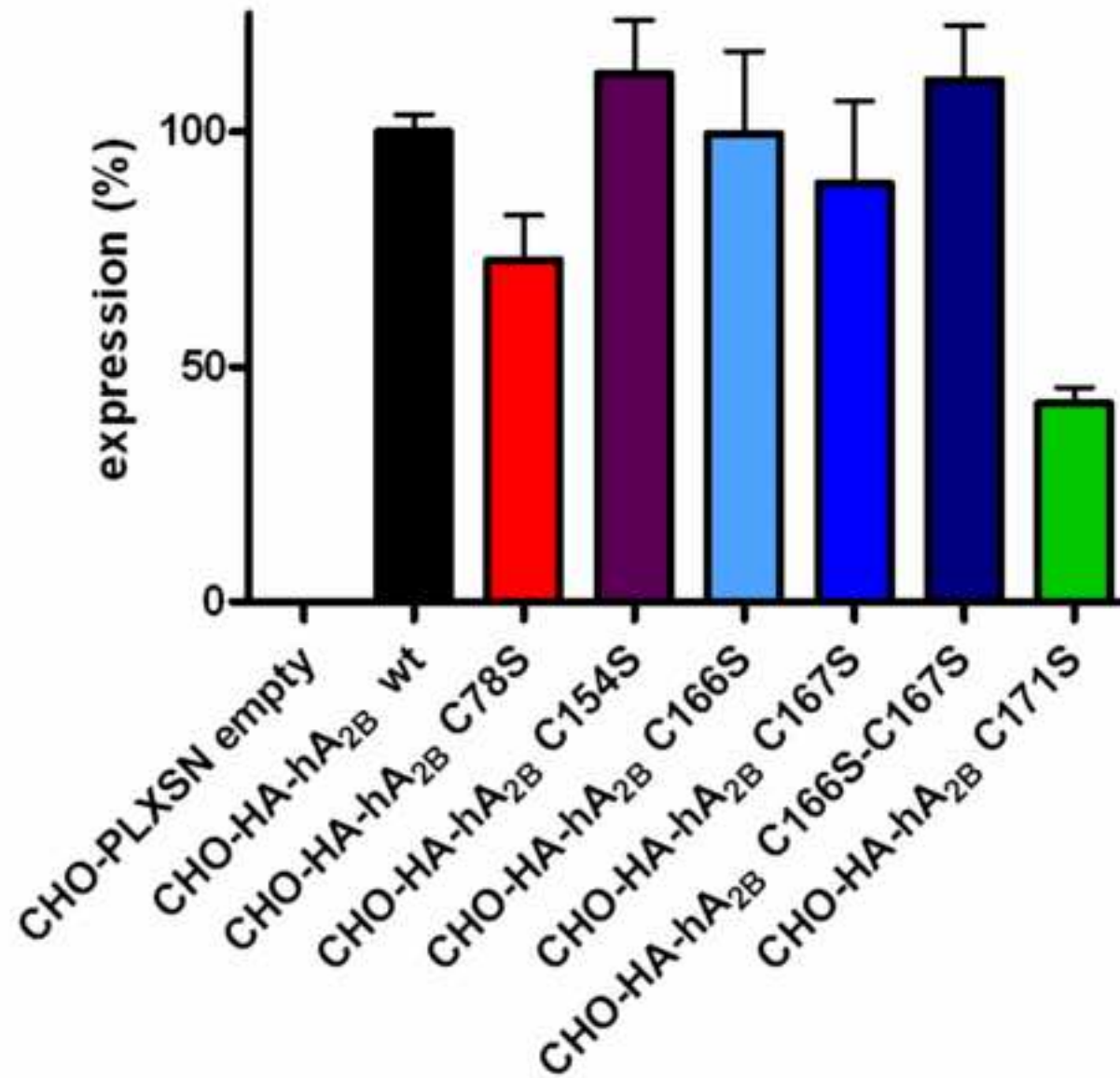
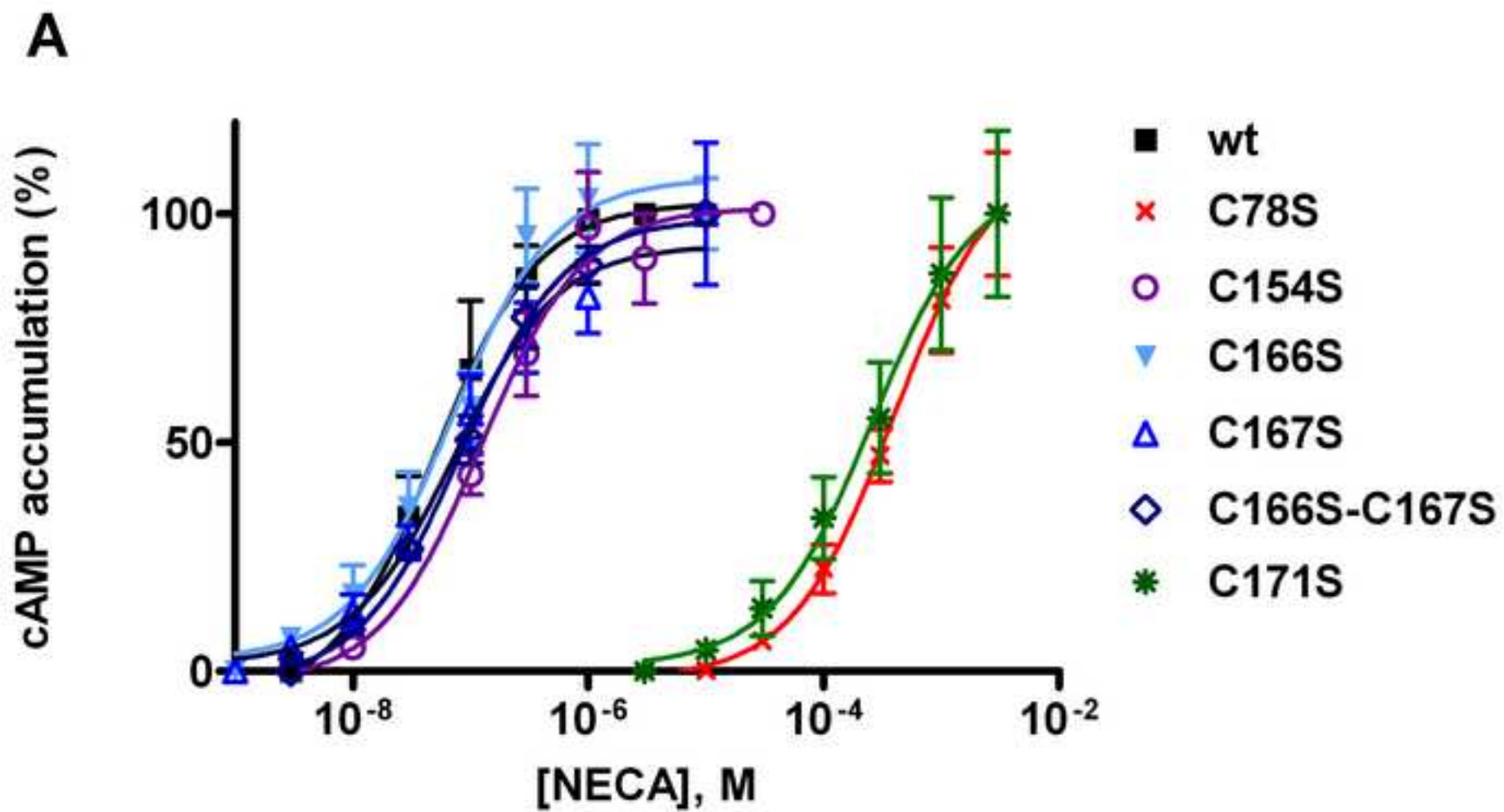


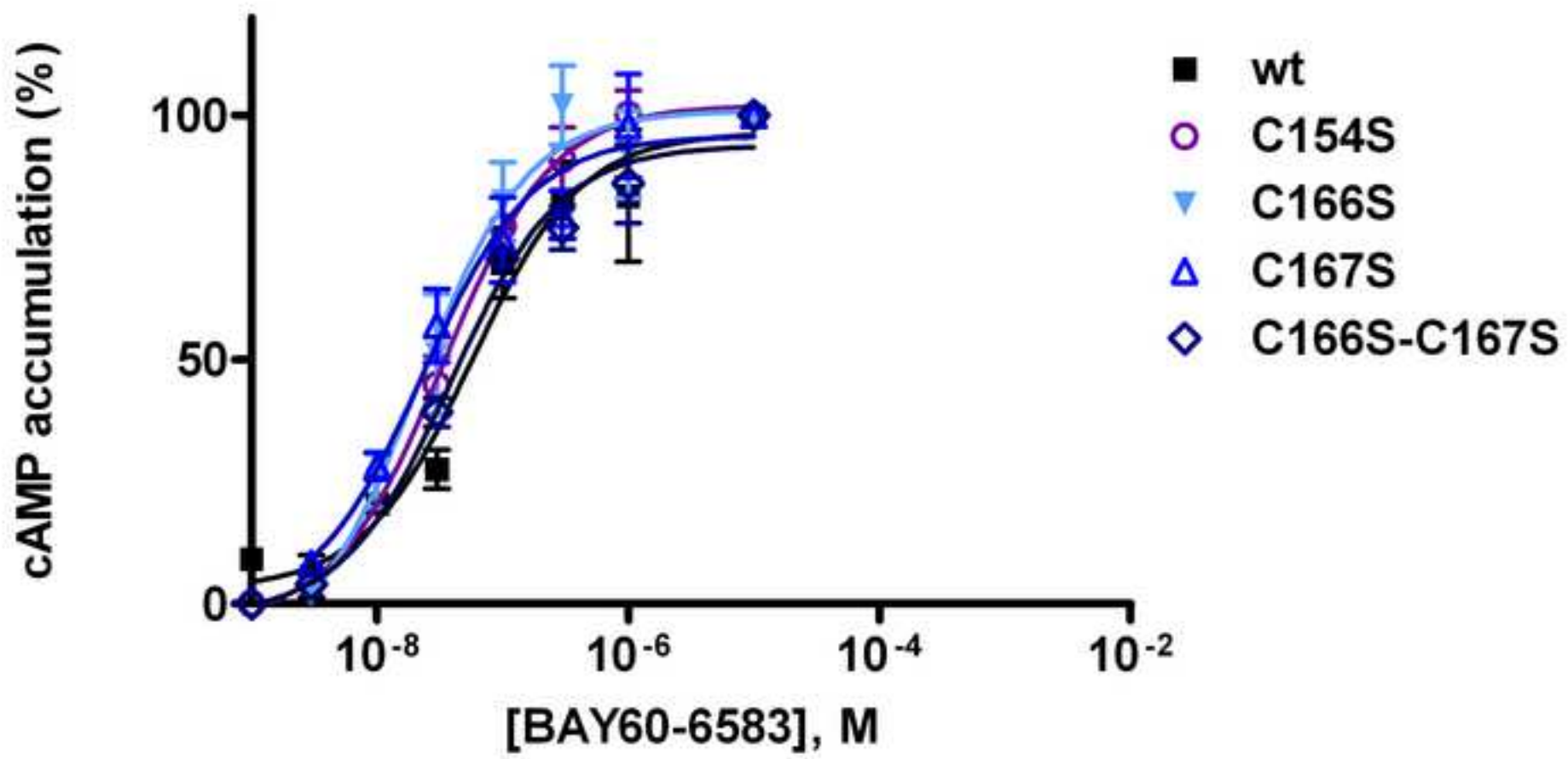
Figure 9
[Click here to download high resolution image](#)

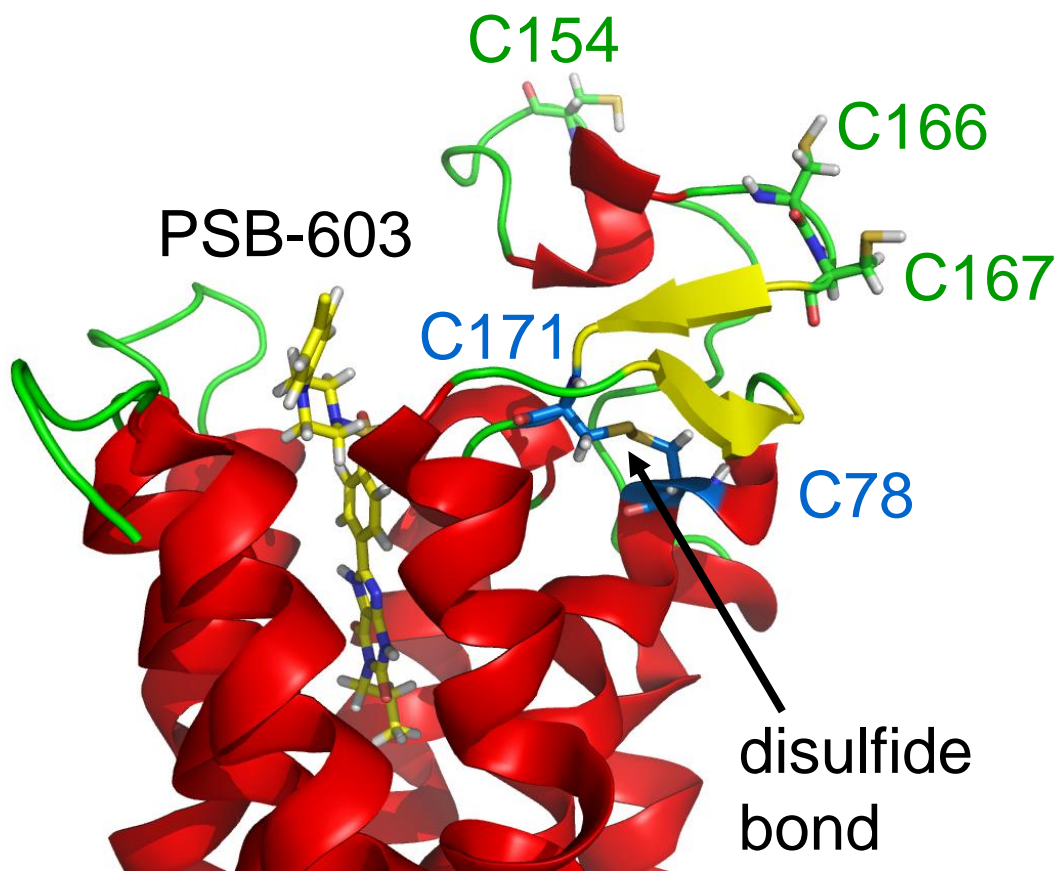




IScrip

B





Adenosine A_{2B} receptors form only **one disulfide** bond between the conserved cysteine residues **C78^{3.25}** and **C171^{45.50}**, the other three cysteines in the loop are not involved in disulfide bond formation.